Environmental
Studies
Research
Funds

077 Analytical Modelling of Oil and Gas Spreading Under Ice

Canada

August 1987

The Environmental Studies Research Funds are financed from special levies on the oil and gas industry and administered by the Canada Oil and Gas Lands Administration for the Minister of Energy, Mines and Resources, and by the Northern Affairs Program for the Minister of Indian Affairs and Northern Development.

Environmental Studies Research Funds

Report No. 077

August 1987

ANALYTICAL MODELLING OF OIL AND GAS SPREADING UNDER ICE

G. Comfort

Arctec Canada Limited,
16, 6325, 11 Street, S.E.,
Calgary, Alberta.
T2H 2L6

Scientific Adviser: R.H. Goodman

The correct citation for this report is:

Comfort, G. 1986. Analytical modelling of oil and gas spreading under ice. Environmental Studies Research Funds Report No. 077. Ottawa.

Published under the auspices
of the Environmental Studies
Research Funds.
ISBN 0-920783-76-7

TABLE OF CONTENTS

	Page
Acknowledgements	(vi)
Summary	1
Resume	3
Introduction	5
Project scope and approach	5
Modelling parameters and interaction processes	6
Spreading mechanisms	6
Under-ice storage capacity	7
Global scale roughness	7
Macro-scale roughness	8
Micro-scale roughness	19
Gas, oil and ice interaction processes	19
Oil and ice	20
Oil and gas	20
Gas and ice	21
Encapsulation	26
Modelling approaches	28
Spreading mechanisms	30
Gas venting	31
Encapsulation	33
Under-ice storage capacity	31
Modelling results	33
Uncertainties and recommendations for future studies	48
References	49
Appendix A: Arctec spreading model program	51

LIST OF TABLES

		Page
1.	Under-ice storage volume summary	11
2.	Ice thickness and standard deviation summary	18
3.	Arctec analysis runs: input values	34
4.	Summary of Arctec analysis results	36
5.	Wotherspoon (1985) model runs: input values	38
6.	Summary of results from Wotherspoon (1985) model runs	39
7.	Comparable run numbers and results for the Wotherspoon (1985) and Arctec models	42

LIST OF FIGURES

Figure		Page
1.	Typical ice thickness profile: Seal Island, Alaska	10
2.	Under-ice storage capacity at Seal Island, Alaska: north-south profiles	12
3.	Under-ice storage volume summary	14
4.	Ice thickness variation at Balaena Bay, NWT	16
5.	Computed and measured under-ice storage volumes	17
6.	Ice sheet failure criteria	23
7.	Spread model flowchart outline	29
8.	Sensitivity of predicted contaminated area to ice roughness	37
9.	Total, upper bound, and lower bound areas of contamination predicted by the Arctec model, Run 2	41
10.	Comparison of Arctec and Wotherspoon (1985) model predictions of contaminated area for a continuous oil spill under smooth ice	43
11.	Comparison of Arctec and Wotherspoon (1985) model predictions of contaminated area for a continuous oil spill under rough ice	44
12.	Comparison of Arctec and Wotherspoon (1985) model predictions of contaminated area for a continuous oil and gas spill under smooth ice	45
13.	Comparison of Arctec and Wotherspoon (1985) model predictions of contaminated area for a continuous oil and gas spill under rough ice	46

ACKNOWLEDGEMENTS

The assistance of Richard F. Brown, who was part of the project team, in completing this study is gratefully acknowledged. Mr. Brown carried out the initial review of the Balaena Bay field discharge tapes and was instrumental in developing the modelling rationale described in this report.

SUMMARY

An evaluation of the recent model developed by Wotherspoon et al. (1985) was performed by undertaking a separate spreading analysis based on the observed processes and on a review of the available literature. This evaluation was done for a spill in the southern Beaufort Sea for the case where currents are negligible. The resulting analysis was used to predict the probable spread of oil and gas under an ice sheet. These results were then compared to the predictions made by the Wotherspoon (1985) model.

The most significant differences between the two approaches are believed to be the treatment of:

° under-ice storage capacity
° a combined gas and oil spill
° ice rupture and gas venting

a) Under-ice storage capacity - the Wotherspoon (1985) model computes the under-ice storage capacity from the input under-ice waveform. Their model considers the under-ice storage capacity to be constant during a run.

In our analysis, the under-ice storage capacity was predicted using observed relations between the under-ice storage and the ice thickness, the ice thickness standard deviation, and the under-ice depression fill depth. This model predicts significantly larger storage volumes than the default values now stored in the Wotherspoon (1985) model.

The available under-ice storage volume is a major uncertainty which limits the accuracy of both analyses. Both approaches involve several assumptions that need to be verified with further research efforts.

b) Combined oil and gas spills - the Wotherspoon (1985) model analyzes this case by multiplying the contaminated area computed for a spill involving oil only with an empirically derived spread factor.

Our analysis was done by considering a combined oil and gas discharge to fill under-ice depressions systematically. This approach also predicts the field data on which the Wotherspoon (1985) model spread factors are based.

c) Ice rupture and gas venting - this oil-gas-ice interaction process is not included in the Wotherspoon (1985) model.

Our model uses Topham's (1980) analysis to predict ice rupture for various ice- and gas-bubble thicknesses.

For oil-only spills, the contaminated areas predicted by the two models compare well after 30 to 40 days have elapsed, provided that comparable under-ice storage capacities are used in both models.

For spills involving both oil and gas, there was a significant discrepancy between the two models. Our analysis predicted large areas of contamination until the ice ruptured, which allowed the gas to vent. The contaminated area is then predicted to reduce very significantly.

In contrast, the Wotherspoon (1985) model predicted that the contaminated area would increase linearly throughout the spill. If ice rupture occurs, smaller areas of contamination are predicted by our analysis for large spills. If ice rupture does not occur, our analysis predicted larger areas of contamination than did the Wotherspoon (1985) model.

The contaminated areas predicted by both models are considered to be subject to great uncertainty. The greatest source of uncertainty is believed to be present knowledge of under-ice storage capacity. Consequently, it is recommended that efforts to map the under-ice surface in three dimensions receive greatest priority.

RÉSUMÉ ADMINISTRATIF

Une évaluation du modèle récent mis au point par Wotherspoon et autres (1985) a été réalisée en faisant une analyse d'étalement distincte, fondée sur les faits observés et sur une étude de la documentation existante. Cette évaluation a été faite pour un déversement dans le sud de la mer de Beaufort, lorsque les courants sont négligeables. L'analyse a été utilisée pour prévoir l'étendue probable du pétrole et du gaz en dessous d'une couche de glace. Ces résultats ont ensuite été comparés aux prévisions énoncées par le modèle Wotherspoon (1985).

Les principales différences entre les deux méthodes semblent être le traitement de:

. la capacité d'accumulation sous la glace;
. un déversement combiné de pétrole et de gaz;
. la rupture de la glace et le dégagement de gaz.

a) Capacité d'accumulation sous la glace - Le modèle Wotherspoon (1985) calcule la capacité d'accumulation sous la glace à partir de la forme de l'onde sour la glace. Il donne une capacité d'accumulation sous-glace constante pendant une coulée donnée.

Dans notre analyse, nous avons prévu la capacité d'accumulation sous-glace, en utilisant les relations observées entre l'accumulation sous-glace et l'épaisseur de la glace, l'écart-type d'épaisseur de la glace, et la profondeur de remplissage de la dépression sous la glace. Ce modèle prévoit des volumes d'accumulation beaucoup plus importants que les taux du modèle Wotherspoon (1985).

Le volume disponible d'accumulation sous-glace est encore très incertain, ce qui limite l'exactitude des deux analyses. Ces deux méthodes donnent lieu à plusieurs hypothèses qui doivent être vérifiées dans le cadre de nouvelles recherches.

b) Déversements combinés de pétrole et de gaz - Le modèle Wotherspoon (1985) analyse ce cas en multipliant la zone contaminée, calculée pour un déversement de pétrole seulement, avec un facteur d'étalement obtenu de façon empirique.

Nous avons, quant à nous, effectué notre analyse en envisageant un déversement combiné de pétrole et de gaz susceptible de remplir systématiquement des dépressions sous la glace. Cette méthode prévoit également les données d'information sur lesquelles les facteurs d'étalement du modèle Wotherspoon (1985) sont fondés.

c) Rupture de la glace et dégagement de gaz - Cette interaction pétrole, glace, gaz n'est pas envisagée par le modèle Wotherspoon (1985).

Notre modèle utilise l'analyse de Topham (1980) pour prévoir la rupture de la glace suivant les diverses épaisseurs de la glace et des bulles de gaz.

Pour les déversements de pétrole seulement, lez zones contaminées indiquées par ces modèles se comparent après 30 à 40 jours, à condition qu'ils utilisent tous deux les mêmes capacités d'accumulation sous la glace.

Pour les déversements de pétrole et de gaz, les deux modèles présentent des différences importantes. Notre analyse prévoit, pour sa part, des zones de contamination importantes jusqu'à la rupture de la glace qui permet un dégagement de gaz. Après quoi, la zone contaminée diminue considérablement.

Pour le modèle Wotherspoon (1985), en revanche, la zone contaminée augmenterait de façon linéaire pendant tout le déversement. En cas de rupture de la glace, notre analyse prévoit des zones de contamination plus limitées pour des déversements importants, et en cas de non-rupture, des zones de contamination plus étendues que celles du modèle Wotherspoon (1985).

Les zones contaminées indiquées par ces deux modèles sont cependant très incertaines. Cette incertitude vient surtout du manque de connaissance actuel de la capacité d'accumulation sous-glace. Nous recommandons, par conséquent, que l'on accorde la priorité à la cartographie en trois dimensions de la surface sous la glace.

INTRODUCTION

Hydrocarbon exploration in ice-infested waters has brought into focus the need to understand the behaviour and fate of oil and gas released in this environment. To this end, many field and laboratory studies have been conducted. With this information, various investigators have attempted to model analytically the interaction of oil and gas with sea ice.

Recently, Wotherspoon, Lewis, Kowalchuk and Armstrong (1985) have developed an analytical model to describe the spread of oil and/or gas under a level ice cover. This project was initially commissioned to supply quantitative calibration data for their model (hereinafter referred to as the Wotherspoon (1985) model).

PROJECT SCOPE AND APPROACH

The proposed project approach was based on the quantitative analysis of field data, in the form of underwater photography, which was collected during large-scale oil-under-ice tests at Balaena Bay, NWT (NORCOR 1975). This approach proved to be impractical as the available field data were largely qualitative in nature. Thus, it was impossible to derive quantitative information that could be used for direct comparison with the Wotherspoon (1985) model. Consequently, it was decided to attempt an evaluation of the Wotherspoon (1985) model by conducting an independent spreading analysis based on the observed processes and on a review of the literature.

Although the Wotherspoon (1985) model was intended to provide a general predictor for the spread of oil and gas under a level ice sheet, our analysis was undertaken specifically for the case of a spill in the southern Beaufort Sea. Significant research efforts have already been expended toward understanding this case, and it is one scenario that the Wotherspoon (1985) model was intended to address. For their model, the output graphics and default input values (e.g., spread factors for a combined oil and gas spill) are based on a spill in this location. The sample run listed in their report was conducted for a spill in the southern Beaufort Sea.

For this oil spill scenario, the physical processes affecting the spread of oil and gas were first assessed. This was done by reviewing underwater photography collected during field oil-under-ice discharge tests at Balaena Bay (NORCOR, 1975) and by reviewing the available literature. A modelling rationale was suggested and probable values for critical parameters (e.g. under-ice storage) were identified. This analysis was used to predict the probable spread of oil or gas or both, under an ice sheet. The results were then compared to the predictions made using the Wotherspoon (1985) model.

MODELLING PARAMETERS AND INTERACTION PROCESSES

This section reviews and discusses the interaction processes and parameters which are considered relevant for modelling the spread of oil and/or gas under an ice cover. These include:

- spreading mechanisms
- under-ice storage capacity
- gas, oil and ice interaction processes
- encapsulation

Each is discussed to provide an understanding of the processes necessary for an accurate spreading analysis.

SPREADING MECHANISMS

The spreading rate and the distribution of oiled ice are believed to be governed by the discharge rate, the under-ice depression fill rate, and the local pattern of under-ice roughnesses. Currents are considered to have only a minor influence on the spread and distribution of spilled oil for the case of a spill in the southern Beaufort Sea. From an analysis of the Balaena Bay photographic data, it was observed that the oil released under an ice cover filled the under-ice depressions systematically. During the offshore test phase of the Balaena Bay test program (which was conducted in the presence of currents up to about 10 cm/s), currents were observed to cause a directional bias. They were, however, too low either to strip oil from under-ice depressions or to restrict lateral spreading of the oil. The final downstream distribution of oil released in the presence of this current was observed to be governed by local roughnesses.

Under-ice current measurements for offshore southern Beaufort Sea sites indicate that currents are likely to be both low, in relation to the current magnitude necessary to cause relative movement of the oil along the ice under-surface, and oscillatory, possibly reflecting tidal patterns (Herlinveaux and de Lange Boom 1975; Cox et al. 1980). The use of a constant current value for these regions is expected to produce misleading results although this may not be true for the Mackenzie Delta region which is affected by the outflow of the Mackenzie River.

The simultaneous release of oil and gas does not appear to alter significantly the basic under-ice spreading mechanisms observed for an oil discharge. The inclusion of gas with the oil, however, may increase the area of contamination, as gas is likely to be released in substantially greater volumes than oil in a blowout condition (NORCOR, 1977).

UNDER-ICE STORAGE CAPACITY

Ice thickness variations occur in nature over a range of scales which may provide significant storage volumes, thereby limiting the spread of oil and gas. Field studies (e.g. NORCOR 1975; Dickins and Buist 1981) have shown that oil or gas released under level arctic ice where currents are low will spread primarily under the influence of gravitational forces. During these tests, the oil and gas systematically filled the under-ice depressions. Consequently, the under-ice relief is significant as it affects the distribution and spread of an oil or gas release by governing the direction of spreading and the depth of accumulation. Consequently, an understanding of under-ice roughness patterns and storage capacity is essential for proper modelling of the spreading of oil and gas under an ice cover.

Under-ice roughness may be categorized generally as follows:

a) **Global-scale roughnesses** such as ridges and rubble fields can create large under-ice storage volumes, provided that they bound level ice areas and that they are sufficiently impermeable to limit or prevent oil migration.

b) **Macro-scale roughnesses** are considered to occur in level ice conditions over areas of tens of square metres and can provide significant storage volumes. Relief features resulting from local thermal regime variations (such as may be induced by local snowdrift patterns) typically occur on this scale.

In thin ice (i.e. less than about 0.5m), under-ice storage may also be provided by rafting features.

c) **Micro-scale roughnesses** are considered to occur over areas less than one square metre. Roughnesses in the skeletal layer of the growing ice sheet occur on this scale.

A discussion of the significance of these under-ice relief types for the modelling of the spread of oil and gas beneath an ice cover is provided in the following subsections.

Global-Scale Roughness

A detailed discussion of global-scale roughness is not possible within the scope of this study. Consequently, only a brief summary is presented.

Global scale roughnesses, such as ridges and rubble fields, have the potential to provide very substantial storage volumes, if they bound level ice areas and are sufficiently impermeable to prevent or limit oil and/or gas migration.

The nature and distribution of global-scale roughnesses is complex and has been the subject of many studies (e.g., Hoare et al. 1980; NORCOR 1978; NORCOR 1977; Comfort and Edwards 1978). Global-scale roughness patterns vary greatly and are highly site-specific. For example, ridge frequencies increase significantly with distance offshore for the Canadian Beaufort Sea throughout the fast ice and transition (shear) zones. Furthermore, global roughnesses vary greatly in composition from poorly consolidated, porous, first-year ridges (which allow the seepage of oil and gas), to highly consolidated, multiyear ridges. Thus, any analytical assessment of the storage volumes provided by these features must be developed specifically for the local study area under consideration.

For the case of a spill in the southern Beaufort Sea, it is believed that global-scale roughnesses are not likely to provide large storage volumes. This area is usually covered with high concentrations of first-year ice. Consequently, most ridges are expected to be relatively unconsolidated and, hence, unable to retain large volumes of oil and gas. Multiyear floes usually comprise a significantly smaller portion of the total ice cover for this area. Thus, there is a relatively low probability that the released oil or gas will contact a zone of ice which is completely bounded by highly consolidated multiyear ridges.

Consequently, we have elected to neglect potential storage volumes provided by global-scale roughnesses for this study.

Macro-Scale Roughness

Macro-scale roughnesses may occur in level ice in response to local thermal regime variations, and in thin ice conditions as a result of rafting processes.

Field observations have shown that rafting generally does not occur for ice thicknesses greater than about 0.5m. The behaviour of oil and gas released in relatively thin ice is not well known. Based on field discharge tests at McKinley Bay, NWT, and subsequent analytical work, Dickins and Buist (1981) noted that gas released under an ice cover of this thickness can be expected to vent quickly. For a spill involving oil only, spreading can be expected to be governed by the under-ice relief, provided that the ice sheet is not broken. If the ice sheet is broken, spreading can be expected to be less extensive as oil is likely to be deposited both under and around the ice block surfaces.

Consequently, emphasis for this study was placed on the analysis of oil spreading under sheet ice conditions. For this ice type, under-ice irregularities formed by local thermal regime variation are believed to provide the greatest storage volume, if the possibility of storage provided by global-scale roughness is excluded.

Under-ice depressions affect the distribution of oil or gas or both under a level ice cover by providing pools and troughs that collect and channel the oil and gas which spreads under the action of gravity and buoyancy forces.

The storage volume available is dependent upon the size and nature of the roughnesses and the depth to which they are filled. Although little data on under-ice roughnesses have been gathered systematically, a number of field measurement programs have been carried out which give some insight into probable under-ice storage volumes. Kovacs et al. (1981) mapped under-ice roughnesses using an impulse radar ice thickness profiler over a variety of level ice conditions near Prudhoe Bay, Alaska. They found under-ice roughness patterns ranging from local "pits" to relatively linear troughs. They computed the under-ice storage volume by assuming that only inter-connected depressions less than the mean ice thickness were filled. Depressions less than the mean ice thickness that were surrounded by areas greater than the mean ice thickness (e.g., local pits) were not included in their storage volume estimates. The storage volume provided by these local pits was small and represented less than 5% of the total area mapped. From this analysis, they found that the oiled ice area would have been about 50% of the total area mapped, if the under-ice depressions are assumed to be filled to the level of the mean ice thickness.

As part of this study, Comfort (1986) collected under-ice roughness data over several profiles for first-year sea ice near Seal Island, Alaska and for freshwater ice at Thunder Bay, Ontario. Figure 1 shows a typical ice thickness profile measured at Seal Island.

Table 1 summarizes under-ice storage volume data from both Kovacs et al. (1981) and Comfort (1986). Table 1 summarizes the relationship between the storage volume and the ice thickness standard deviation that has been measured over a wide range of locations and ice conditions. These data indicate that the under-ice storage capacity may range from 33% to 103% of the ice thickness standard deviation for the case where the under-ice depressions are filled to the level of the mean ice thickness.

Figure 2 shows the variation of storage volume with depression fill depth ratio. Comfort (1986) found that the storage volume increased greatly as the pools were filled to greater depth. He measured an exponential increase in storage capacity, to about the 2.7 power with increasing fill depth ratio.

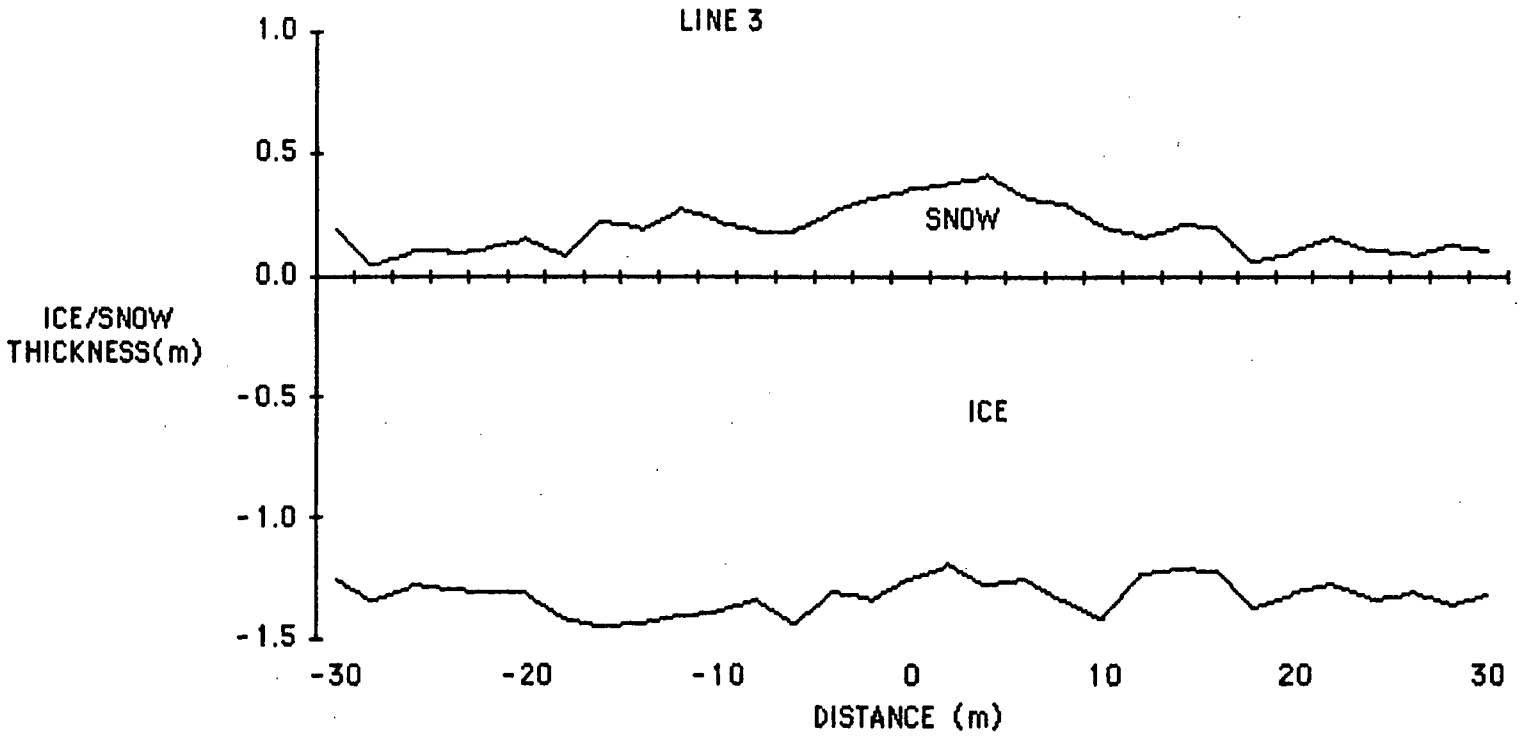

Figure 1. Typical ice thickness profile: Seal Island, Alaska (after Comfort 1986).

TABLE 1
Under-ice storage volume summary

Location	Mean ice thickness (m)	Ice thickness s.d.[3]	Storage Volume (m^3/m^2)	Storage volume Ice thickness s.d.[3]	Comments
[1]Tigvariak Is. aircraft runway	1.55	0.031	0.032	1.03	150-m long profile
[1]West Dock site	1.83	0.150	0.0605	0.40	Avg. of area with uplifted ice block to 0.15 m over 127 m x 160 m grid
[1]Reindeer Is. flat smooth ice	1.33	0.010	0.010	1.00	Est. only from sessile drop theory
[1]Site A	1.52 - 1.53	N/A[4]	0.0237 - 0.0254 Avg. = 0.0248		Range over 220-m long legs of equilateral triangle
[1]Site B	1.57 - 1.61	N/A	0.0209 - 0.0264 Avg. = 0.0239		Range over 220-m long legs of equilateral triangle
[1]Site C	1.57 - 1.60	N/A	0.0452 - 0.0574		Range over 220-m long legs; data may be unreliable because of "slush keels"
[2]Seal Island, Alaska	1.19 - 1.26	0.049-0.092	0.10 - 0.220 Avg. = 0.130	1.50 - 2.90	Depressions completely filled range over 6, 60-m profiles
			0.017 - 0.036 Avg. = 0.023	0.33 - 0.39	Depressions filled to mean thickness level; range over 6, 60-m profiles
[2]Thunder Bay harbour	0.79 - 0.83	0.038-0.063	0.065 - 0.110 Avg. = 0.022	1.50 - 1.90	Depressions completely filled; range over 6, 60-m profiles
			0.014 - 0.025 Avg. = 0.022	0.38 - 0.41	Depressions filled to mean thickness level; range over 6, 60-m profiles

[1] Kovacs et al (1981)
[2] Comfort (1986)
[3] s.d. = standard deviation
[4] N/A = data not available

Note: Kovacs et al (1981) computed the storage volume by assuming that only inter-connected under-ice depressions less than the mean ice thickness were filled.

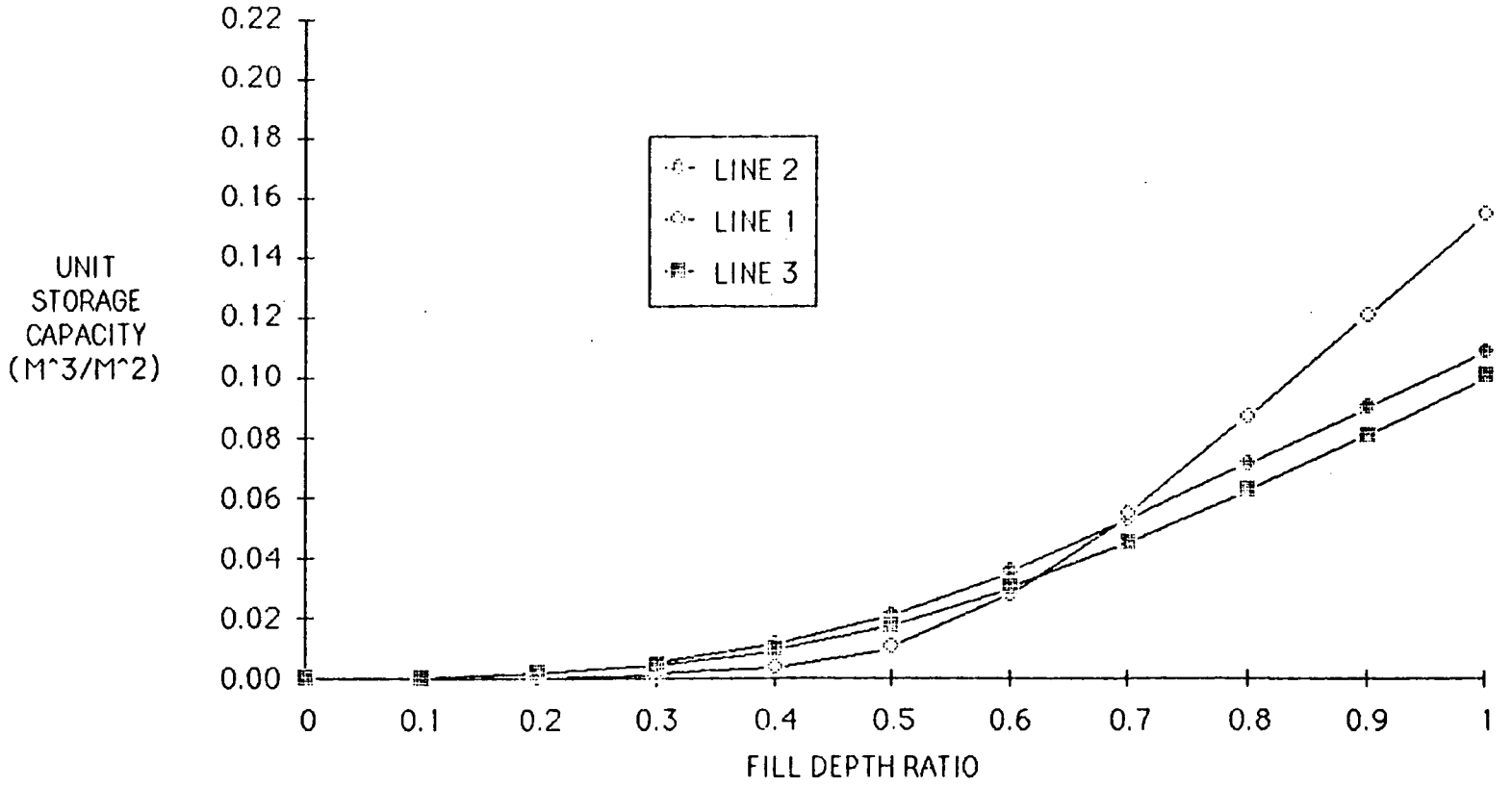

Figure 2. Under-ice storage capacity at Seal Island, Alaska: north-south profiles (after Comfort 1986).

This relationship may be summarized as follows:

Storage volume = [a dimensional constant] x fill depth ratio $^{2.7}$

where the fill depth ratio is defined as:

$$\frac{\text{max. distance from ice surface to interface between water and oil or gas} - \text{minimum ice thickness}}{\text{maximum ice thickness} - \text{minimum ice thickness}}$$

It can be seen that the assumed fill-depth ratio is highly significant.

It is believed that the Kovacs et al. (1981) analysis underestimates the available storage volume. For a large spill it is probable that there will be an encompassing boundary that is deeper than the mean that will cause increased flooding in the interior. Also, as will be outlined in the subsection on encapsulation, an encompassing ice lip has been observed to form around the spilled oil in response to local thermal gradients at the edge of the oil lens. As these pools must now fill to greater depth to flood the ice lip before further spreading is possible, it is expected that the under-ice depressions will be filled closer to the maximum storage level for a large spill. For this study, the under-ice storage volume was first bounded by assuming two levels of storage corresponding to fill-depth ratios of 0.5 and 1.0. Subsequently, this analysis was refined by considering the initial under-ice storage to be the above lower bound value and then to allow the storage to increase as oil and gas were added to the system. As will be discussed in the section on modelling, this approach predicts that the fill depth ratio will approach a value of unity for large spills.

The available storage volume data have been collected for relatively thick ice ranging from about 1.2 to 1.8 m (excluding the freshwater ice data set for which the mean thickness was about 0.8 m). The available storage volume over the ice growth cycle is of interest for modelling the spread of oil and gas under a level ice cover.

Figure 3 shows that the storage volume increases slightly with increasing thickness and indicates a significantly larger storage volume at Kovacs et al. (1981) West Dock site than at the other sites. This is believed to reflect local conditions at that site where significant storage volume was provided by a refrozen lead.

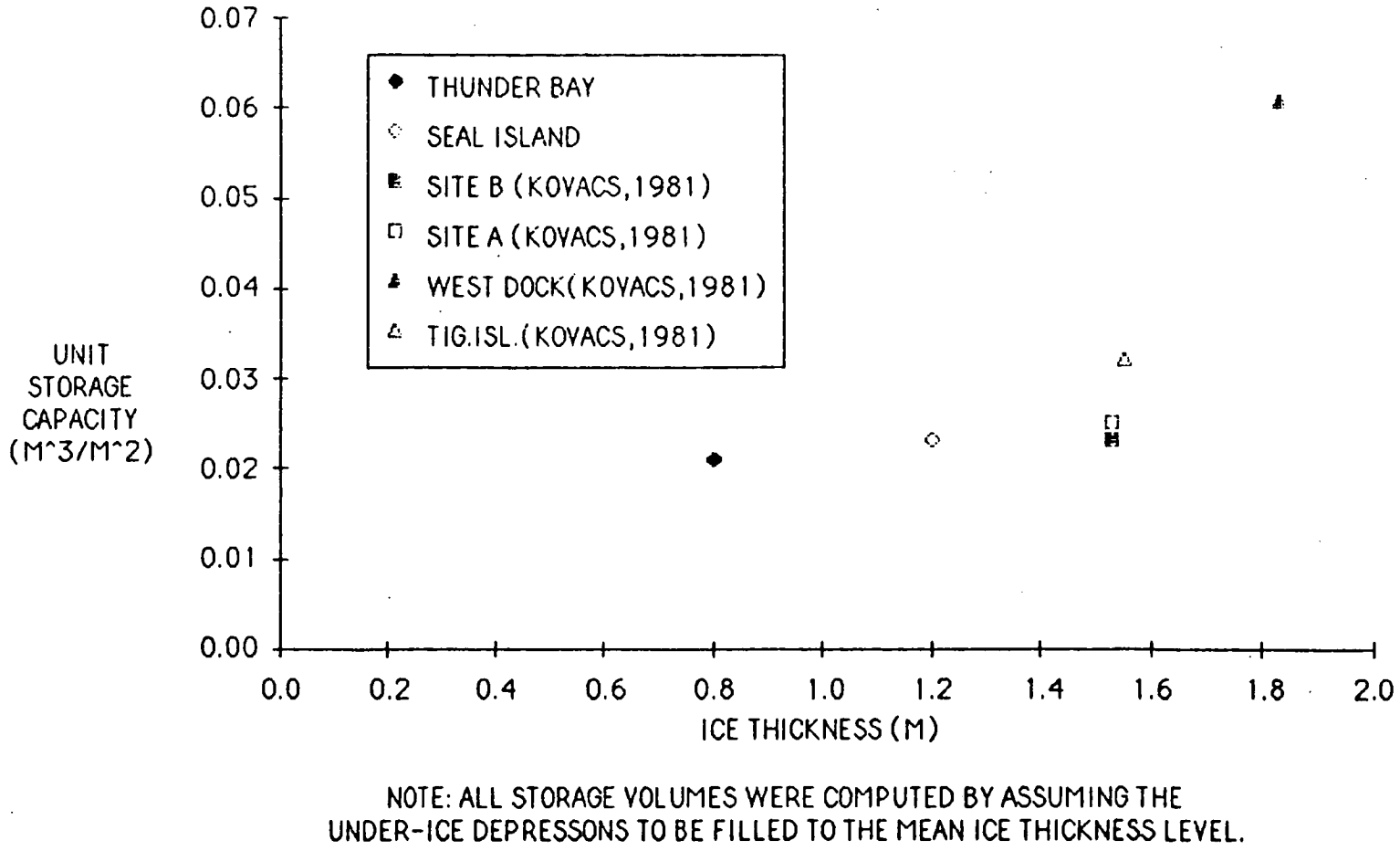

Figure 3. Under-ice storage volume summary.

Figure 4 shows ice thickness variation data collected at Balaena Bay, NWT (NORCOR, 1975) during the complete ice growth cycle. This figure indicates that the ice thickness variation and, hence, the storage capacity, is essentially a linear function of the mean ice thickness once the sheet exceeds about 60 cm.

From a comparison of Figures 3 and 4, it is not clear that the under-ice storage capacity is strongly related to the ice thickness. In an attempt to obtain further understanding, the under-ice storage was computed (using the approach described in Figure 5) for Balaena Bay, and Viscount Melville Sound (Comfort 1978) ice roughness data sets (see Figure 5). The computed storage capacities show reasonable correlation with the measured storage capacities in relation to the ice thickness. Additional field data are required to resolve this issue definitively. For this study, we have elected to assume that the under-ice storage capacity increases linearly with the ice thickness for ice thicknesses greater than 0.5 m.

The local ice and snow conditions are expected to influence the under-ice storage capacity. The under-ice storage is likely to be related to the ice thickness standard deviation, which is expected to reflect the under-ice roughness. Table 2 summarizes the relationship of the mean ice thickness to its standard deviation as measured over a range of ice conditions. The data indicate that the ice thickness standard deviation may range from 0.1% to 15.8% of the mean ice thickness.

The Tigvariak Island data were collected along an aircraft runway which was clear of snow and consequently, may not be representative of ice conditions in the southern Beaufort Sea. For the West Dock site, significant storage was provided beneath a refrozen lead so this data set is expected to overestimate the storage volume to ice thickness standard deviation ratio for ice conditions in the southern Beaufort Sea.

If these anomalous data points are neglected, then the range of measured storage volume to ice thickness standard deviation ratios reduces to 0.33 to 0.41.

From this discussion, it can be seen that the under-ice storage volume is an area of significant uncertainty. For this study, the following assumptions were employed to estimate the under-ice storage volume for sheet ice in excess of 0.5 m in thickness.

a) The under-ice storage volume was assumed to increase linearly with the ice thickness.

b) The under-ice storage volume was taken as 30% of the ice thickness standard deviation when the under-ice depressions were filled to the mean ice thickness level. This assumption errs conservatively in that the under-ice storage volume is underestimated.

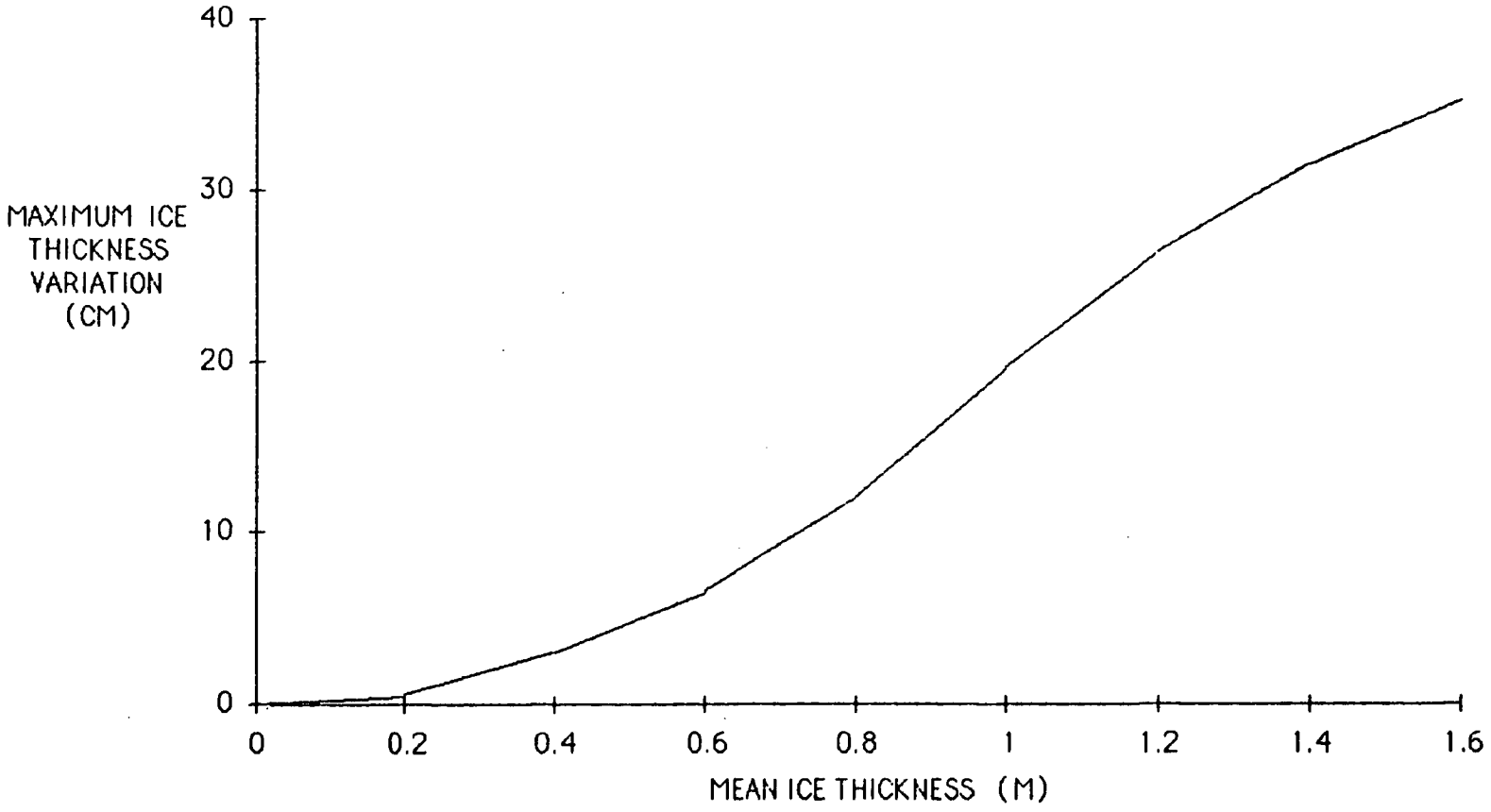

Figure 4. Ice thichness variation at Balaena Bay, NWT (after NORCOR 1975).

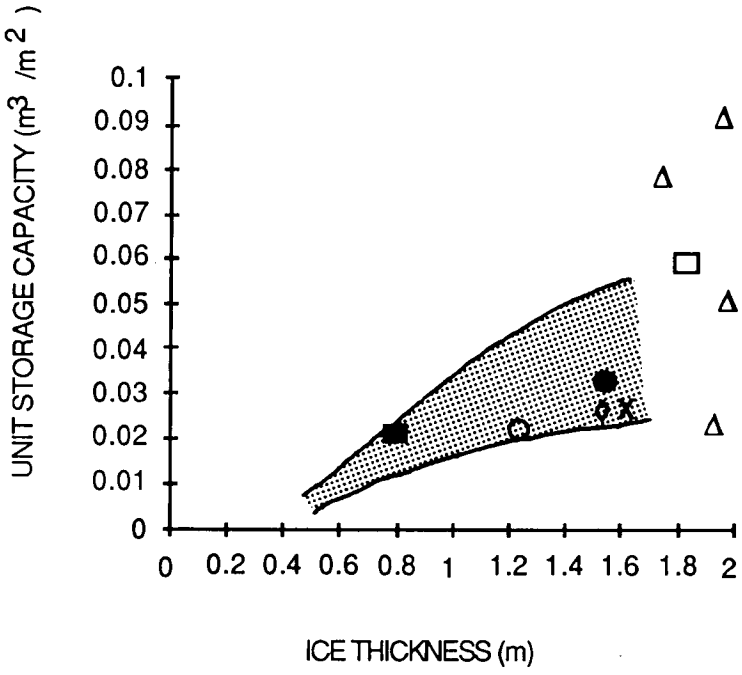

MEASURED VALUES

- ■ Thunder Bay (Comfort, 1986)
- O Seal Island (Comfort, 1986)
- ◊ Site A (Kovacs, 1981)
- X Site B (Kovacs, 1981)
- □ West Dock (Kovacs, 1981)
- ● Tigvariak Island (Kovacs, 1981)

COMPUTED VALUES

- Δ Viscount Melville Sound (Comfort, 1978)
- ▨ Balaena Bay, NWT (Norcor, 1975) - see note #2

Notes:

1. All storage volumes were computed by assuming the under-ice depressions to be filled to the mean ice thickness level.

2. Storage volumes at Balaena Bay were computed by assuming that the reported ice thickness variation ranged from two to four ice thickness standard deviations.

Figure 5. Computed and measured under-ice storage volumes.

TABLE 2

Ice Thickness and Standard Deviation Summary

Source	Location and snow/ice conditions	Mean ice thickness	Ice thickness std. dev.	Percentage of mean value	Comments
Comfort 1986	Thunder Bay harbour: smooth ice conditions w/snowdrifts to 0.1 m	0.787 - 0.825	0.038 - 0.063	4.8 - 7.9	Range for 6, 60-m profiles
	Seal Island, Alaska: smooth ice conditions w/snowdrifts to 0.6 m	1.19 - 1.26	0.049 - 0.092	4.1 - 7.6	Range for six profiles
Kovacs et al 1981	Tigvariak Island: aircraft runway w/snow removed	1.55	0.031	2.0	
	West Dock site: ice surface roughnesses to 0.15 m with snow drifting around uplifted ice	1.83	0.150	8.0	Average over 127 m x 160 m grid; significant storage was provided by a refrozen lead
	Reindeer Island: flat smooth ice	1.33	0.010	0.1	
Comfort 1978	Viscount Melville Sound: snowdrifts to 0.6 m and uplifted ice features to 0.15 m	1.75 - 1.98	0.080 - 0.310	4.2 - 15.8	Range of values over four profiles, each 25+ km long

c) Two cases of ice roughness were considered. The ice thickness standard deviations were taken as 5% and 15% of the mean ice thickness.

d) The under-ice depressions were assumed initially to fill to the level of the mean ice thickness, which corresponds to a fill depth ratio of 0.5. As additional oil and gas were added to the system, the under-ice pools were filled more completely, reflecting the growth of a local ice lip around the oil.

Micro-scale Roughness

Micro-scale roughnesses are considered to occur over areas less than a square metre. Ice skeletal layer roughnesses occur over this scale and have the potential to provide storage. The Wotherspoon (1985) model incorporated a range of default under-ice relief conditions that are representative of skeletal layer roughnesses. These roughnesses provided a range of storage volumes from 0.007 to 0.027 m^3/m^2.

The significance of ice skeletal layer roughnesses is unclear. Very little oil was entrapped in the skeletal layer during field tests conducted at Balaena Bay, NWT (NORCOR 1975). During these tests, the oil appeared to etch or erode a channel in the skeletal layer and repeatedly followed the same course at it flowed in "rivulets" to the nearest dome under the ice. A different behaviour was observed during late-winter tests at McKinley Bay, NWT (Dickins and Buist 1981) in which the oil filled some of the voids in the ice skeletal layer.

Additional research work is required to resolve this issue. For this study it was decided to neglect storage volumes in the ice skeletal layer as their role is uncertain. This assumption errs conservatively (in that the available storage volume is underestimated). However, as probable macro-scale storage volumes are significantly greater than ice skeletal layer volumes, this assumption is not expected to result in large errors.

GAS, OIL, AND ICE INTERACTION PROCESSES

This subsection reviews the interaction processes relevant to spreading which occur when oil or gas or both are released under a static, level ice cover. These processes are complex and depend on the interaction of all three components. For simplicity, the following discussion has been organized into a description of the component interactions in three parts.

Oil and Ice

The release of oil under a level ice cover has been studied in some detail in both the laboratory and the field. The largest field program conducted to date involved a series of controlled discharges under static ice conditions during the complete ice growth cycle at Balaena Bay, NWT (NORCOR, 1975). Most tests were conducted in a sheltered bay where currents were negligible, although one test took place offshore where currents up to about 10 cm/s were present.

From the tests conducted, a good understanding of the oil-under-ice spreading process has been gained. Underwater photography collected during the Balaena Bay tests showed that the oil flowed along under-ice troughs in "rivulets" to the nearest dome under the ice where it pooled. Little oil was entrapped in the skeletal layer and in the immediate vicinity of the plume. The oil appeared to etch a channel in the skeletal layer and repeatedly followed the same course. Thus, the oil filled the macro-scale under-ice depressions systematically as it spread under the influence of gravitational forces. Both currents and gravitational forces influenced oil spreading in the offshore test.

Currents were found to cause a directional bias in the distribution of oil. During the offshore tests, NORCOR (1975) found that the oil travelled at about half the current speed and that the majority of the oil was deposited downstream of the discharge point. However, the currents at the site were too low either to strip oil from the domes or to restrict lateral movement of the oil. The downstream distribution of the oil was governed by the local under-ice roughness patterns.

During laboratory tests, Cox et al. (1980) found that current velocities in the range of 15 to 25 cm/s were necessary to cause movement of the oil relative to the ice surface. Currents of this magnitude are not generally present in the southern Beaufort Sea during the ice-covered period. Herlinveaux and de Lange Boom (1975) found under-ice currents to be low. They conducted measurement programs at two locations in the southern Beaufort Sea and found under-ice currents were typically less than 3 cm/s. Furthermore, the currents were oscillatory, possibly reflecting tidal patterns. Consequently, a significant directional bias is not expected. Therefore, for this study we have elected to analyze the zero-current case.

Oil and Gas

A simultaneous release of oil and gas under blowout conditions is expected to involve large volumes of gas in relation to oil (NORCOR, 1977). An understanding of the final configuration of oil and gas under the ice cover is necessary for modelling the spread of oil and gas.

Oil and gas discharge tests of limited duration were conducted at McKinley Bay (Dickins and Buist 1981). These tests showed that the oil and gas will rise to the ice-water interface in a turbulent plume, with the oil being broken into large numbers of small droplets ranging in diameter from tens of microns to 2 mm.

For the December tests, oil and gas were deposited under the ice in discrete oil droplets and gas bubbles with a coating of oil. The ice bottom in areas without gas was uniformly coated with small oil droplets which penetrated and seemed to adhere to the skeletal layer.

For the April and May discharges, oil and gas were deposited in the under-ice depressions as pools of oil overlain by gas pockets. For these tests, it was observed that the oil moved easily along the ice surface and that the oil and gas moved along the ice under-surface to fill the available depressions.

All of these tests involved discharges of short duration (i.e., less than one hour). Consequently, it is necessary to make some assumptions regarding the oil and gas configuration for large spills. It is believed that spreading would occur predominantly under the influence of gravitational forces for a large spill as the bulk of the oil and gas would be removed from the effects of the plume. Therefore, for this analysis, we have assumed that the oil and gas may be considered to fill the under-ice depressions as pools of oil overlain by gas.

Gas and Ice

The behaviour of oil and gas released beneath an ice cover has been studied in the field (Dickins and Buist, 1981) and in the laboratory (e.g., Purves, 1978; Kisil, 1980). These studies provided considerable insight into the gas-ice interaction process, although significant uncertainties still remain.

Venting, dissipation and ice erosion are aspects of the gas-ice interaction process which need to be considered for the modelling of the spread of oil and gas beneath an ice cover.

Venting

The hydrostatic force of the trapped gas may fracture the ice cover, thereby allowing a large proportion of the gas to escape to the atmosphere (Dickins and Buist, 1981). This condition will affect the spread of oil under the ice, as gas is expected to be released in significantly larger volumes than oil.

The fracture of an ice sheet by a trapped gas bubble, and its subsequent venting, has been observed in the field (Dickins and Buist 1981). For thick ice, large gas bubbles are required to cause failure and it is not clear whether rupture will occur. Dickins and

Buist (1981) have speculated that ice more than 1 m thick is unlikely to rupture. In addition, the presence of leads and other major flaws in the ice sheet may serve to vent the released gas.

A simple elastic analysis using thin-plate theory has been proposed by Topham (1977) to model the deflection and fracture of an ice sheet under hydrostatic loading by a trapped gas bubble of uniform depth. Topham's analysis predicted failure criteria (i.e., critical gas bubble depths and radii) for ice sheets of given thickness and mechanical properties. Depending on the configuration of the gas bubble, failure of the sheet may occur either at the centre or at the edge of the bubble (Figure 6). As the bubble depth was decreased, the analysis predicted greatly increased spread radii to cause failure, and it seems likely that failure would not occur for thick ice with thin bubble films.

Topham's analysis suffers from a number of inaccuracies. Most important, he did not consider the mechanical properties of the ice to be time-dependent. Field and laboratory tests (e.g. Mellor 1983) have shown that ice creep is significant under low strain-rate loadings (such as would be the case for a trapped gas bubble) and, hence, long-term deflections are significantly greater than short-term values.

The results of Topham's analysis showed reasonable correlation to the McKinley Bay field tests (Dickins and Buist 1981) in which the trapped gas bubble cracked the 0.59-m ice sheet along the bubble periphery over about 20-m radius. Using Topham's 1977 analysis and the same ice mechanical properties that produced the data in Figure 6 (after Topham 1980), a uniform gas bubble depth of 6.1 cm was predicted to cause failure. As the measured ice thickness standard deviation was only 3.90 cm, a unit storage capacity of only 0.012 to 0.039 m^3/m^2 would be expected for this ice (see subsection on macro-scale roughness). However, the mean ice thickness for the ruptured area was 3.9 cm less than the mean value for the Phase I study area. As this was a zone of thinner ice, it is expected that the under-ice depressions would be filled to a level greater than the mean thickness value. As the unit storage capacity increases greatly with increasing fill depth, the failure criterion predicted by Topham's 1977 analysis was within the range of probable values.

Unfortunately, the McKinley Bay field test cannot be relied upon for corroboration of Topham's 1977 model because ice failure occurred soon after the gas was released. Consequently, little creep strain is expected to have occurred in the ice during this test and, therefore, an elastic representation of the ice mechanical behaviour is likely to provide reasonable accuracy.

Considerable effort would be required to extend Topham's analysis to the case of a long-term blowout. Non-linear stress analyses, which take into account material visco-elastic properties, are possible but involve significant computing. Also, there is con-

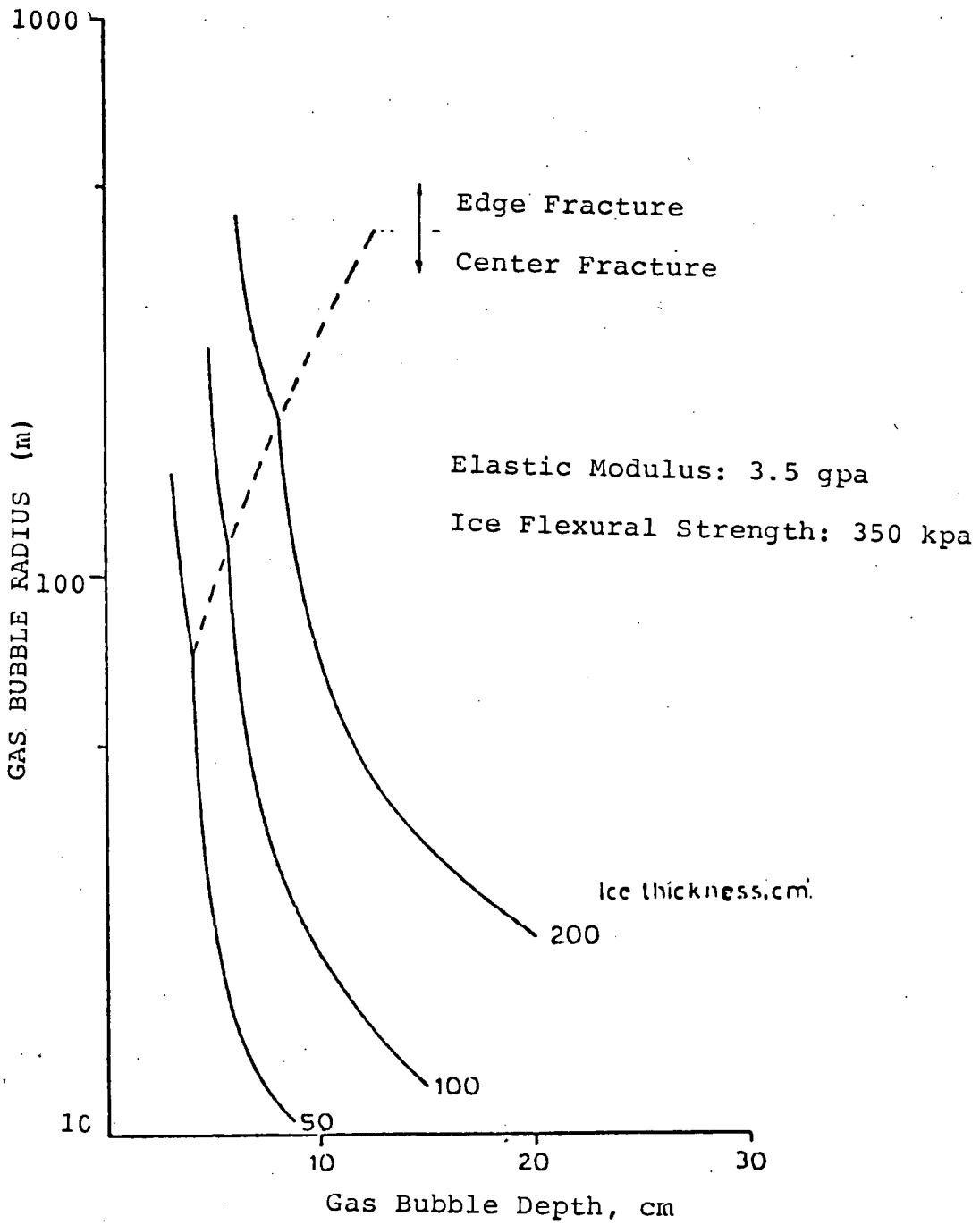

Figure 6. Ice sheet failure criteria (after Topham 1980).

siderable uncertainty regarding the ice mechanical properties under long-term loadings. If effective values of ice flexural modulus (reflecting long-term loading cases) were input into Topham's model, it might be possible to use his analysis for long-term loadings.

However, when reduced values of the ice elastic modulus are used, Topham's analysis predicted that substantially increased bubble depths would be required to cause failure. This result contrasts with field ice-bearing capacity tests that have been done, which show that the long-term bearing capacity is significantly less than the short-term strength. These tests have shown the long-term ice-bearing capacity is limited by large ice deflections that cause cracking and flooding.

In summary, Topham's 1977 analysis is considered to provide reasonable accuracy for cases in which ice rupture occurs quickly (i.e., within about one hour) after the gas is released. For longer-term loadings, Topham's model will err conservatively in that it will overestimate the resistance of the ice sheet to failure which will produce an overestimate of the spreading for spills involving oil and gas. Consequently, we have used his model for this preliminary study.

After fracture of the ice cover occurs, venting of the gas will commence through the cracked ice sheet. The gas flow-rate under these conditions will determine the volume of gas that is vented to the atmosphere and, hence, the quantity of oil and possibly gas that must be stored under the ice sheet. In turn, this venting rate will influence the area of contamination.

The available field data from McKinley Bay (Dickins and Buist 1981) provide some indication of gas flow rates in fractured ice conditions. In Phase I, holes representing about 0.3% of the area above the gas discharge point were drilled in the ice sheet. These were estimated to be sufficient to vent about 80% of the released gas and indicated a gas flowrate through the broken ice of about 150 m^3/m^2 per day.

At this rate of venting, the stored gas would be released quickly to the atmosphere. Considering that the storage capacity of the level ice is expected to reach only about 0.5 m^3/m^2 then clearly all the gas not encapsulated under the ice sheet, would be vented in one day.

For large contaminated areas, complete venting may not occur if ice rupturing is localized and, consequently, it may not be possible for all of the gas stored in the under-ice depressions to reach the cracked ice. In addition, ice rupture may not occur immediately and some gas may become encapsulated in the ice (see later subsection). On the other hand, the ice sheet may progressively fail after initial cracking and eventually release most of the gas stored beneath the ice cover.

This is an area of uncertainty. For our analysis, we have assumed that most (i.e. 80%) but not all of the gas will be vented. It is expected that this will produce a conservative spreading estimate.

Dissipation. If venting does not occur, the released gas will pool beneath the ice cover. Laboratory and field data indicate that the pooled gas will then become encapsulated in the growing ice sheet. The release timing and mechanism is somewhat unclear, although the available data indicate that the gas will dissipate through the warming ice sheet through microscale cracks and brine channels, and will surface before the oil is released.

Purves (1978) conducted laboratory experiments to investigate the release timing of oil and gas discharged under, and encapsulated in, a saline ice sheet. He found that the gas bubbles remained incorporated in the ice sheet until the ice temperature reached -3.6°C. The gas subsequently dissipated to the ice surface at a steady-state rate of about 1.5×10^{4} m^3/m^2 per day. With further warming of the ice sheet, the encapsulated oil was released by migration through brine channels.

Kisil (1980) conducted similar experiments and also found that dissipation of the encapsulated gas occurred only under warm ice conditions. In these tests, gas release commenced over a range of ice temperatures from -2.2°C to -6.0°C.

These tests indicate that the process of gas dissipation is ice-temperature-dependent and that gas dissipation does not occur until the ice is relatively warm. They indicate a low dissipation rate, implying that gas dissipation will not significantly affect the spread and distribution of oil and gas under an ice cover.

Dickins and Buist (1981) conduced field oil and gas discharge tests at McKinley Bay that have provided some additional information; however, they noted that gas dissipation requires further investigation. Some cores taken in June at the Phase 2 and 2A discharge sites showed the presence of air voids, indicating that air was encapsulated in the ice by the growing ice sheet. Therefore, the process of gas dissipation was not likely to have affected the spread and final distribution of oil and gas at these sites significantly as both the oil and the air was encapsulated in the ice sheet.

Consequently, it is expected that gas dissipation will not greatly affect the spread of oil and gas under an ice cover. This process could be modeled analytically using the available laboratory data. Gas dissipation, however, should be included only as part of a spreading model for warm ice conditions.

Ice erosion. Depending on the thermal conditions at the blowout site, the gas, oil, and water plume may have the thermal capacity to erode the under-ice surface near the blowout point. If this were

sufficient to initiate failure of the sheet and, hence, venting of the gas, then the spread of oil in relatively thick ice conditions (where venting did not occur quickly) could be reduced to a great extent.

The probable importance of ice erosion processes can be assessed using plume theory (e.g., Milgram 1983) and stagnation point heat transfer theory (e.g., Topham 1975). Topham[1] indicated that, for probable blowout conditions, the entrainment of water can be expected to be the most significant factor affecting the thermal capacity of the plume. Therefore, the temperature profile of the water is of great significance for an assessment of ice erosion potential. For the southern Beaufort Se, several field measurement programs (e.g., Herlinveaux and de Lange Boom 1975) have shown that winter water temperature profiles are nearly isothermal at the freezing point. Therefore, there is little heat available in the water column to drive the ice erosion process. Consequently, it is expected that the ice erosion process will not greatly affect the spreading of oil and gas under an ice cover in the southern Beaufort Sea. For this reason, this factor has not been included in our analysis.

ENCAPSULATION

Oil discharge tests under an ice cover at Balaena Bay, NWT (NORCOR 1975) and oil and gas discharge tests under an ice cover at McKinley Bay, NWT (Dickins and Buist 1981) have shown that encapsulation of the pooled oil and gas is an important process affecting their spread. During these tests the discharged oil and gas was rapidly incorporated into the growing ice sheet. At Balaena Bay, the discharged oil was encapsulated in the ice sheet after only one day, for all tests except the mid-May discharge. (For this test, oil surfaced through the brine channels within one hour). The mean oil-film thickness was 2.1 cm and the ice growth rate did not exceed about 1 cm/day. Therefore, it can be seen that oil-film thicknesses significantly greater than the ice growth rate were encapsulated in a one-day period.

At McKinley Bay, Dickins and Buist (1981) observed that, for the December discharge, almost all of the oil and gas bubbles were encapsulated by a 1-cm layer of new ice in one day. It should be remembered that, for these tests, most of the discharged gas was vented through the ice sheet. For the April tests, a period of 48 hours was required to encapsulate the oil and gas, including an air-filled trough 20 to 25 cm deep. For the May discharge, it was possible to conduct only one survey dive 24 hours after the release occurred. At that time, only small oil globules had frozen in. For these tests, the natural ice growth was estimated not to exceed 1 cm/day.

---

[1] D. Topham, Institute of Ocean Sciences, Sidney, B.C., personal communication, 1985.

During laboratory experiments, Kisil (1980) also observed the formation of an ice lip around an oil or gas bubble released under an ice cover. When the ice lip reached the depth of the oil or gas, horizontal ice growth occurred, encapsulating the bubble. Ice then continued to grow vertically at a reduced rate, as compared to the control case. Over the range of gas and oil bubble depths studied (i.e., 1.1 to 2.1 cm) and gas-to-oil ratios tested (i.e., 4 to 17), the ice growth for the control case was measured to be 1.9 to 2.5 times greater than that for the oiled ice case over an approximate two-day period after discharge. The formation of an ice lip effectively immobilizes the discharged oil or gas or both (NORCOR 1975) and contributes to increased storage, as the under-ice depressions must fill to greater depth before further spreading is possible.

Encapsulation is, therefore, an important consideration. Further information is required for accurate modelling as there are uncertainties regarding the effect of a continuous spill on the encapsulation process. From the available information, however, it is believed that the effects of encapsulation processes may be incorporated into a spreading model for low-current cases by allowing an ice lip to grow around the oil or gas which increases the available storage to a maximum when all the depressions are completely filled. The rate of growth of the ice lip is dependent upon the ice growth rate in the absence of oil and gas, the depth and area extent of the oil or gas, and the ratio of oil and gas. The field data indicate an ice-lip growth rate of at least twice the control ice growth rate. For our analysis, we have adopted this value, as it errs conservatively by overestimating the spreading that will occur.

MODELLING APPROACHES

In the previous section a number of modelling parameters were identified for the various processes that affect the spread of oil or gas or both, under an ice cover. A simple spreading model has been developed and was run over a range of input values to provide comparative data for the Wotherspoon (1985) model. Appendix A provides a listing of the BASIC computer program.

Figure 7 illustrates the model flowchart in general terms.

The spreading model has the following input parameters:

- initial ice thickness and standard deviation;
- ratio of the unit storage capacity to the ice thickness standard deviation;
- oil flow rate and gas-to-oil ratio;
- rate of gas dissipation through the ice sheet and the ice thickness at which gas dissipation commences;
- proportion of gas volume that is released when venting occurs;
- ice flexural strength (for ice rupture check);
- ratio of the ice growth rate of an ice lip around the spilled oil and gas to the unoiled ice-growth rate;
- storage capacity increase exponent for increasing fill-depth ratios; and
- unoiled ice growth rate.

After entering these parameters, the model stepped through a series of calculations to determine the total volume of oil and gas under the ice sheet and the contaminated area. The under-ice storage capacity was initially taken as a linear function of the ice thickness standard deviation. For oiled ice areas, the storage capacity increased with fill depth ratio to a maximum when the pools were filled to the maximum level.

For simultaneous oil and gas releases, checks were made using Topham's 1977 analysis for ice rupture. If venting occurred, the volume of gas was reduced. Gas dissipation through the intact ice sheet was considered although it was allowed to occur only for warm ice conditions.

Our modelling approach is compared with the modelling approach developed by Wotherspoon (1985) in the next four subsections.

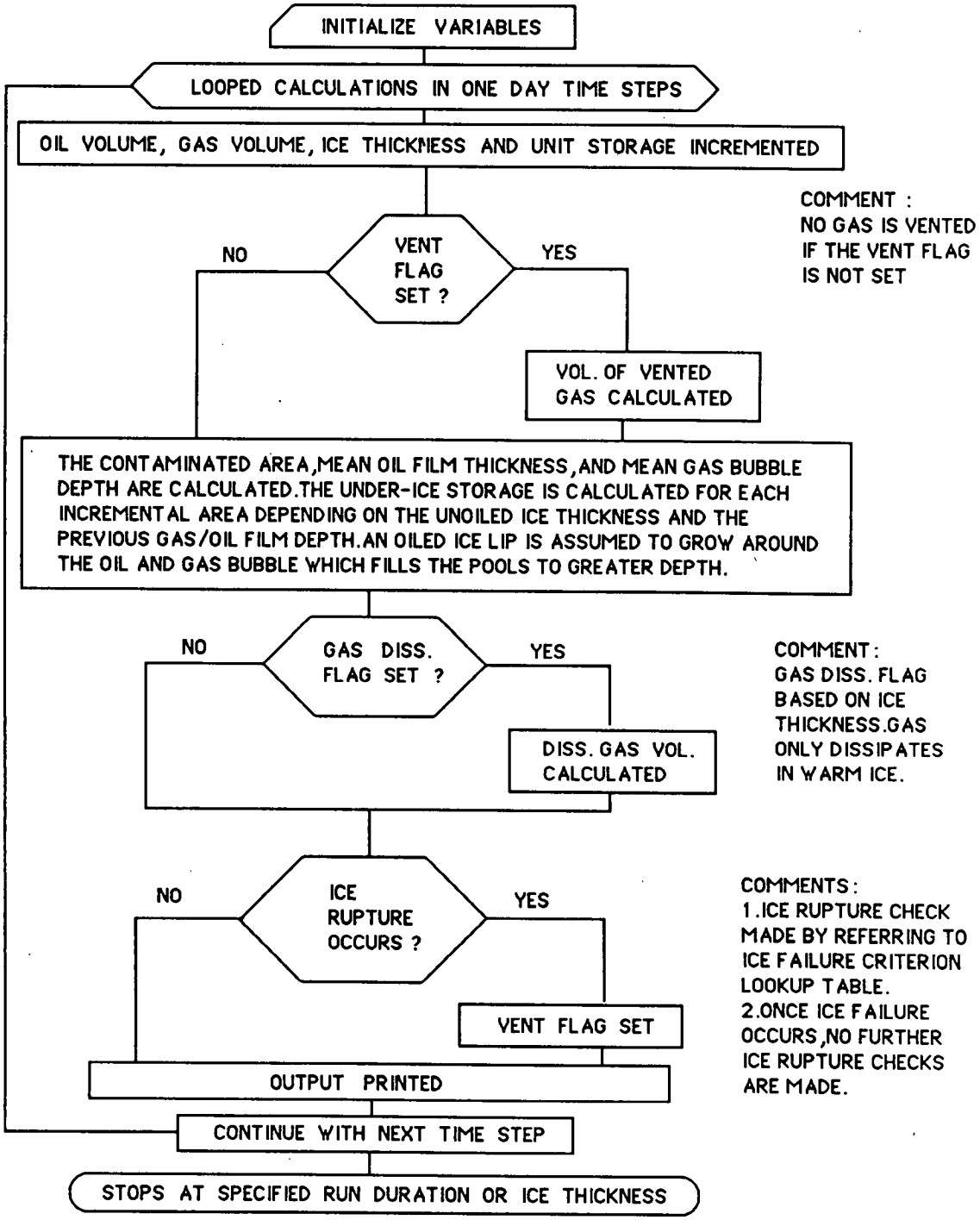

Figure 7. Spread model flowchart outline.

SPREADING MECHANISMS

Without Currents

In the absence of currents, both models allow the oil and gas to fill the under-ice depressions systematically under the action of gravitational forces.

The Wotherspoon (1985) model permits the oil to fill the under-ice depressions completely and then to pool to its equilibrium slick thickness before spreading further. Our analysis considers the oil pool initially to the mean ice thickness level and subsequently to fill the under-ice depressions to a greater depth, as the local ice growth is modified by the presence of the oil and gas. Because the equilibrium slick thickness is small, this additional storage was excluded in our analysis.

For large spills, our analysis predicts that the depth of the oil in pools will approach the maximum ice thickness level. Therefore, little difference is expected between the two models for large spills, provided that equivalent under-ice storage capacities are used.

As the Wotherspoon (1985) model was intended to provide a general treatment of the spread of oil or gas, or both, under an ice sheet, the effect of currents on the oil distribution was included in their model. The effect of currents was neglected in our specific calculation for a spill in the southern Beaufort Sea. The likely significance of this modelling variation is discussed in more detail later.

For spills involving both oil and gas, the Wotherspoon (1985) model calculated the area of contamination by computing the area for the oil-only case and then multiplying it by an empirically-derived spread factor to account for the presence of the gas. This spread factor was based on one set of field observations at McKinley Bay (Dickins and Buist 1981) and was therefore, specific to those prevailing oil and gas discharge flowrates and ice conditions (i.e., thickness and roughness). Consequently, this approach lacks rigour and reduces the versatility of their model. This approach also makes the treatment of gas-only discharges difficult.

For spills involving oil and gas, or gas only, our analysis was done by assuming the oil or gas to fill the under-ice depressions systematically (and similarly to the oil-only case). This approach also predicts the field data on which the Wotherspoon (1985) model is based.

With Currents

The effect of currents on oil-under-ice spreading has not been included in our model, which was conducted specifically for the case of a spill in the southern Beaufort Sea. This effect was excluded because offshore under-ice currents are expected to be unsteady and low, relative to the current magnitude necessary to cause relative oil-ice movement (e.g., Herlinveaux and de Lange Boom 1975; Cox et al 1980).

The Wotherspoon (1985) model was intended to be of more general use and, consequently, included the effects of currents on the distribution of oil and gas in other geographic areas.

As the comparative runs for these two models were conducted for the zero-current case, this difference is not expected to produce a significant discrepancy.

GAS VENTING

Gas venting is not considered to occur in the Wotherspoon (1985) model and thus their model would be expected to predict significantly larger areas of contamination for spills involving both oil and gas. However, as will be shown in the next section, the Wotherspoon (1985) model predicts lower areas of contamination than does our analysis for a combined oil and gas discharge occurs. This results from their use of empirically-derived spread factors which limit the spread of oil and gas in the system. In their model, the spread factor is about 28 times less than the gas-to-oil ratio (for a gas-to-oil ratio of 200).

ENCAPSULATION

The Wotherspoon (1985) model considered all oil slicks not moved by currents to be encapsulated; thus, for the zero-current case, all of the oil will be encapsulated.

Our approach includes the effects of encapsulation by taking into account the resulting modified storage.

UNDER-ICE STORAGE CAPACITY

The under-ice storage capacity was calculated from input values for both models. The Wotherspoon (1985) model used as input the size of the under-ice roughness whereas our analysis was based on observed relations between the ice thickness, the under-ice pool fill depth, the ice thickness standard deviation, and the ice storage capacity. As outlined previously, our analysis considered that the storage capacity increased as the pools become filled to greater depth.

At present the Wotherspoon (1985) model has a range of default storage capacities from 0.005 to 0.027 m^3/m^2. These default storage capacities are considerably less than measured values for the southern Beaufort Sea (as discussed previously). Consequently, these default values are believed to underestimate the under-ice storage for a typical location in the southern Beaufort Sea. Therefore, larger storage values were used in the Wotherspoon (1985) model to provide runs that could be compared with the results of our analysis.

The Wotherspoon (1985) model considers the under-ice storage to be constant over the run duration. Our analysis allows the under-ice storage to increase as the ice thickness increases and as the under-ice depressions become filled more completely.

MODELLING RESULTS

Our analysis was first conducted for field data collected during the oil and gas discharge tests under sea ice at McKinley Bay, NWT (Dickins and Buist 1981). During this program, the Phase 2 and 2A tests showed that the area of contamination was reduced by 65% when the gas-to-oil ratio was reduced from 180 to 25, or from 224 to 66 if air blow back is taken into account (Dickins and Buist 1981). For these tests, the mean ice thickness and standard deviation were 1.64 $\pm$ 0.06 m and 1.82 $\pm$ 0.087 m, respectively. Using these values, our analysis predicts contaminated area reductions of 70% and 57% for the range of possible gas-to-oil ratios. This correlation between the observed field data and the predictions from our analysis was encouraging.

Our analysis was then run for a number of input values given in Table 3 and for constants as follows:

- run duration: 60 d
- oil flow rate: 1,900 m^3/d
- ratio of under-ice storage to ice thickness standard deviation:[1] 0.30
- ratio of local oiled ice-lip growth rate to unoiled ice growth rate: 2
- proportion of gas volume vented when ice rupture occurs: 0.8
- ice flexural strength: 350 kPa
- storage capacity increase exponent for increasing fill depth ratio: 2.7
- gas dissipation rate:[2] 1.5×10^{-4} $m^3/m^2/d$
- ice growth rate:[3]

---

1 Discussed in subsection on under-ice storage capacity

2 Input as the laboratory test value measured by Purves (1978) and assumed to occur only when ice thickness exceeded 1.75 m. Thus no gas was allowed to dissipate for runs made since they were terminated after 60 days duration.

3 Over the 0.5 to 1.8-m thickness range, ice growth was represented by a penta-linear function based on Banke's observed ice-growth cycle for the southern Beaufort Sea (Dickins and Buist 1981).

TABLE 3

Arctec analysis runs: Input values

Run no.	Gas-to-oil ratio	Initial ice thickness[a] (m)	Ice thickness std. dev. (% of mean thickness	Under-ice storage capacity[b] (m^3/m^2)	
				Start of run	End of run
1	0	0.8	1	.016	.026
2	0	0.8	5	.078	.13
3	0	0.8	15	.23	.38
4	200	0.8	5	.078	.13
5	200	0.8	15	.23	.38
6	0	1.2	5	.12	.16
7	0	1.2	15	.35	.48
8	200	1.2	5	.12	.16
9	200	1.2	15	.35	.48

[a] The ice thickness was considered to be normally distributed and the maximum ice thickness was taken as being 2 standard deviations greater than mean value.

[b] Under-ice storage computed by assuming under-ice depressions to be completely filled.

The results predicted by the model are summarized in Table 4. Figure 8 shows the results for runs 2 and 3.

Two areas of contamination (i.e., the active and total area of contamination) are shown on this figure, and are defined as follows:

- active area of contamination - the area of ice being oiled by each daily discharge: and

- total area of contamination - the total area of ice which has been contaminated up to the point in time being considered.

Our analysis predicts a contamination cycle in which the oil or gas or both, is initially spread over a large area. Subsequently, the total area remains constant until the under-ice depressions become more completely filled. Because the under-ice storage increases more rapidly than does the discharged oil volume, the active area is predicted to decrease initially during the cycle.

Figure 8 also shows the area of contamination to be highly sensitive to the ice thickness standard deviation, and, hence, to the under-ice storage capacity.

The Wotherspoon (1985) model was run for a similar range of input values (Table 5) and for constants as follows:

° spill date: 84-12-15
° run and spill duration: 60 d (1,440 h)
° spill latitude: 69.9 deg. N
° spill longitude: 134.2 deg. W
° oil flow rate: 1,900 m^3/d
° water specific gravity: 1.025
° current velocity: 0
° cross-sectional cavity shape: rectangular
° oil type: 2
° spill type: continuous

Table 6 summarizes the predicted values.

Because of variations in approach between our analysis and Wotherspoon (1985) model, it was not possible to perform comparative runs which were exactly duplicate. In our analysis, the under-ice storage increased both as the under-ice depressions become more completely filled and as the ice thickness increased, whereas the under-ice storage remained constant throughout the run in the Wotherspoon (1985) model. Consequently, separate runs were made for the Wotherspoon (1985) model which bounded the range of under-ice capacities used in our analysis for a single run.

TABLE 4

Summary of Arctec analysis results

Run no.	Initial ice thickness (m)	Ice thickness std. deviation (% of mean thickness)	Gas-to oil ratio	Maximum contamination	
				Area (m2/106) of contamination[a]	Time (days) of maximum contamination[a]
1	0.8	1	0	4.7	60
2	0.8	5	0	1.2	60
3	0.8	15	0	0.5	60
4	0.8	5	200	62.6	3
5	0.8	15	200	10.5	1
6	1.2	5	0	1.1	60
7	1.2	15	0	0.4	60
8	1.2	5	200	71.3	7
9	1.2	15	200	7.0	1

[a] For a run duration of 60 days and oil flow rate of 1,900 m^3/d.

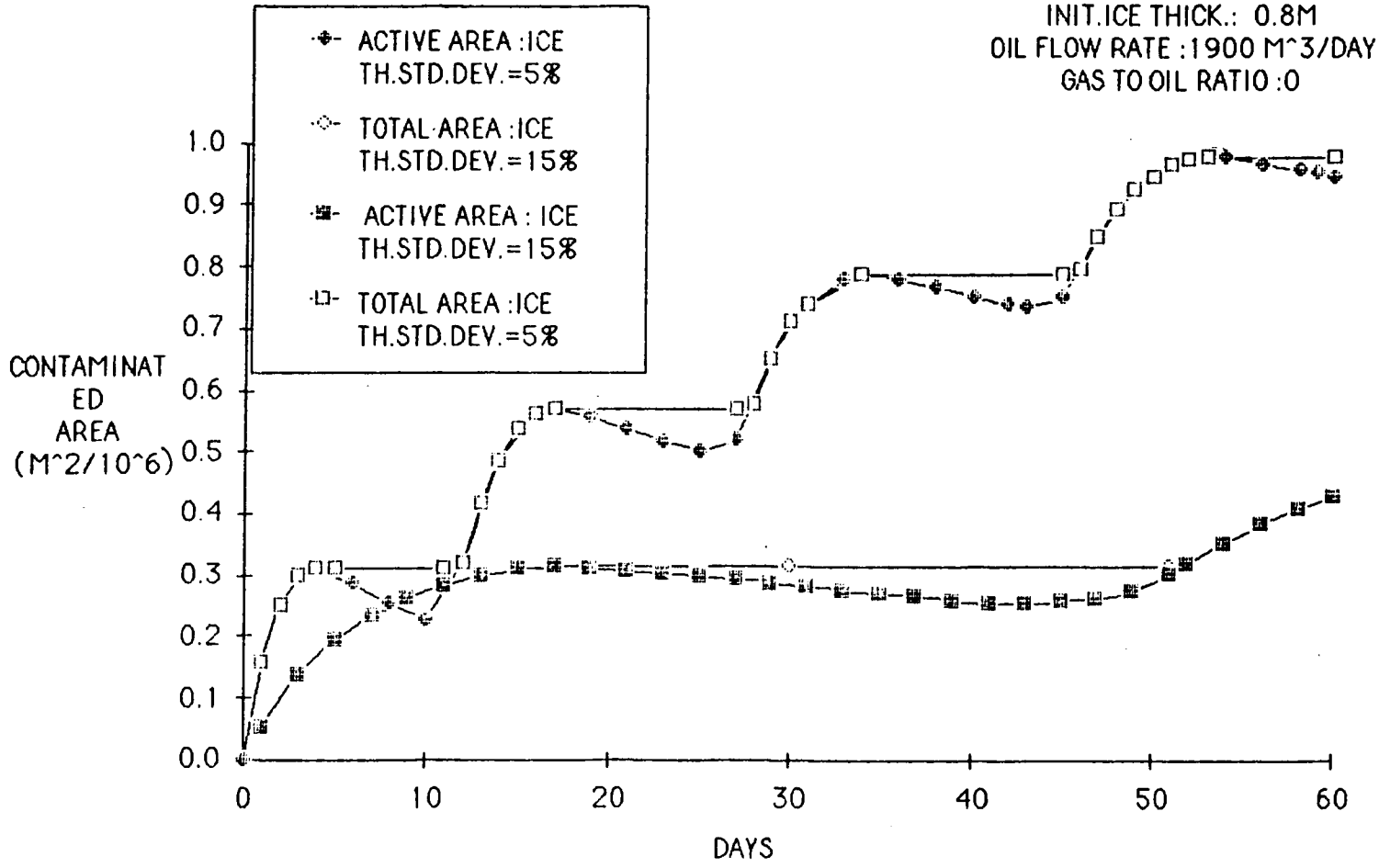

Figure 8. Sensitivity of predicted contaminated area to ice roughness.

TABLE 5

Wotherspoon (1985) model runs: Input values

Run no.	Gas-to-oil ratio	Cavity depth (m)	Cavity width (m)	C-C cavity spacing (m)	Under-ice storage capacity (m^3/m^2)
1	0	0.10	0.78	1.0	0.078
2	0	0.30	0.78	1.0	0.23
3	200	0.10	0.78	1.0	0.078
4	200	0.30	0.78	1.0	0.23
5	0	0.20	0.64	1.0	0.13
6	0	0.60	0.64	1.0	0.38
7	200	0.20	0.64	1.0	0.13
8	200	0.60	0.64	1.0	0.38

TABLE 6

Summary of results from Wotherspoon (1985) model runs

Run no.	Gas-to oil ratio	Predicted area ($m^2/10^6$) of contamination[a]	Time (days) of maximum contamination[a]
1	0	1.4	60
2	0	0.5	60
3	200	9.6	60
4	200	3.3	60
5	0	0.9	60
6	0	0.3	60
7	200	6.0	60
8	200	2.1	60

[a] For a run duration of 60 d and oil flow rate of 1,900 m^3/d.

Our analysis considered the under-ice depressions to fill initially to the mean ice thickness level and then to greater depth, reflecting the growth of a local ice lip around the oil or gas in the depression. This sequence results in a significant increase in under-ice storage. Figure 9 compares the contaminated area predicted by our analysis for Run 2 (see Table 3) with contaminated area predictions obtained by assuming that the under-ice depressions were filled to the mean and maximum ice-thickness levels. This analysis predicted that, for large spills, the fill-depth ratio will approach unity.

Consequently, in an attempt to duplicate as closely as possible the storage volumes used in both models for the comparative runs, input cavity sizes for the runs made using the Wotherspoon (1985) model were selected to provide the same storage capacity as would be predicted by our analysis for a fill depth ratio of unity. Table 7 lists the comparable runs and compares the results obtained.

Figures 10 and 11 compare the contaminated areas predicted by the two models for a continuous oil-only spill under smooth and rough ice. The predicted contaminated areas compare well after 40 days have elapsed. Our analysis predicts higher areas of contamination during the first 40 days especially under rough ice. This discrepancy results from differences in the under-ice storage computation methods. In our analysis the storage capacity increases during the run as the depressions become completely filled. In the Wotherspoon (1985) model the storage capacity remains constant and the under-ice voids are considered to be completely filled after the initial discharge. Storage capacities for the comparative model runs were selected for the case when the under-ice depressions were completely full. Hence, the storage volumes during the initial portion of the run in our analysis were less than the corresponding values given by the Wotherspoon (1985) model.

Figures 12 and 13 compare the contaminated areas predicted by the two models for a continuous spill during which both oil and gas are released under smooth and rough ice. There are significant discrepancies in the predictions obtained from the two models. Our analysis predicted much larger areas of contamination until ice rupture occurred. For rough ice (with an ice-thickness standard deviation equal to 15% of the mean ice thickness), rupture was predicted to occur within the first day. For smoother ice (with an ice-thickness standard deviation equal to 5% of the mean ice thickness), rupture was predicted not to occur until the fourth day which reflects the additional time required to fill the under-ice pools in excess of the mean ice thickness. This delay greatly increased the area of contamination.

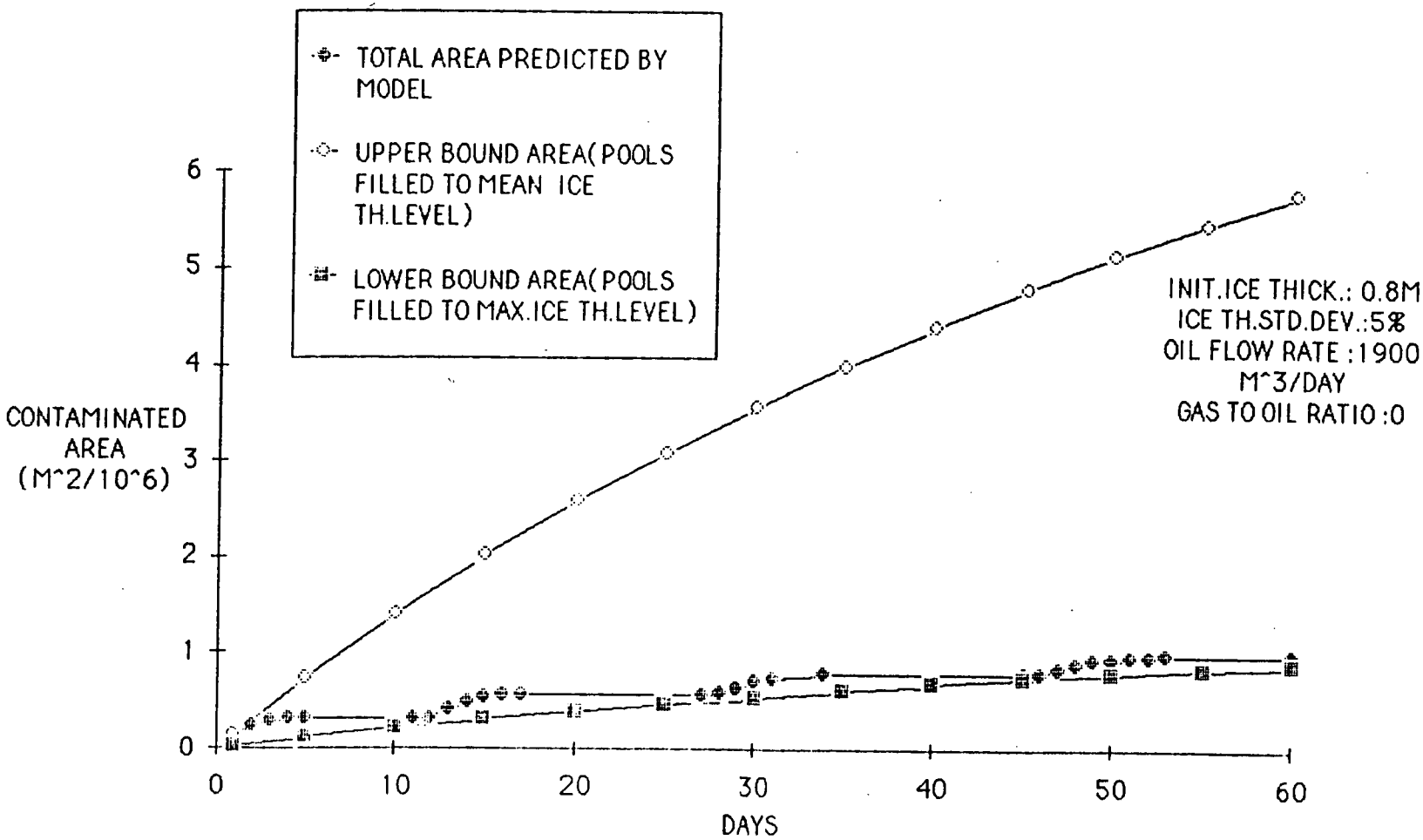

Figure 9. Total, upper bound, and lower bound areas of contamination predicted by the Arctec model, Run 2

TABLE 7

Comparable run numbers and results for the Wotherspoon (1985) and Arctec models

Run no.[a]	Arctec model: Maximum contaminated area ($m^2/10^6$)	Wotherspoon (1985) model: Upper area bound		Wotherspoon (1985) model: Lower area bound	
		Run no.[b]	Max. contam. area ($m^2/10^6$)	Run no.[b]	Max. contam. area ($m^2/10^6$)
2	1.2	1	1.4	5	0.9
3	0.5	2	0.5	6	0.3
4	62.6	3	9.6	7	6.0
5	10.5	4	3.3	8	2.1

[a] see Table 3.

[b] see Table 5.

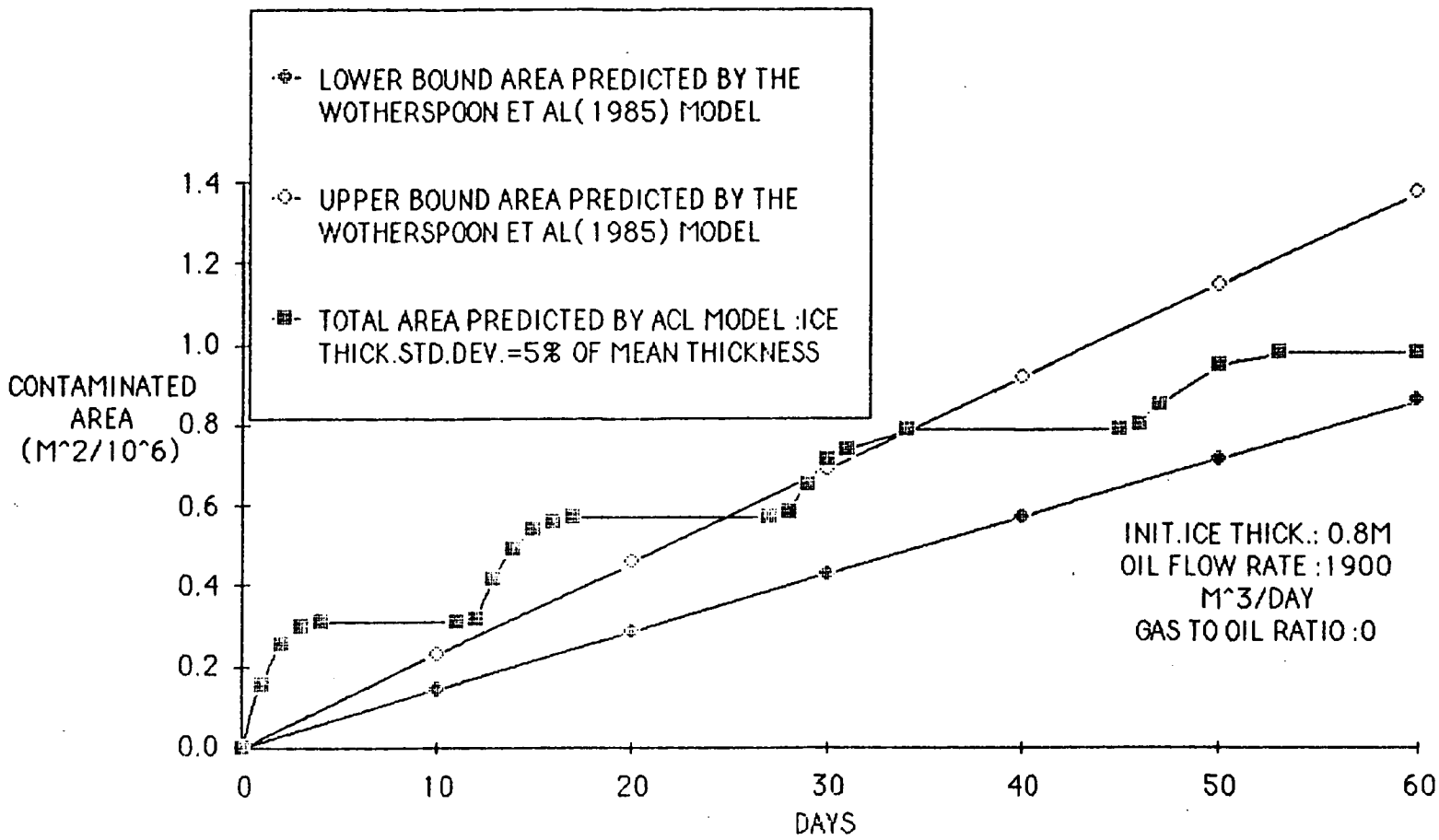

Figure 10. Comparison of Arctec and Wotherspoon (1985) model predictions of contaminated area for a continuous oil spill under smooth ice.

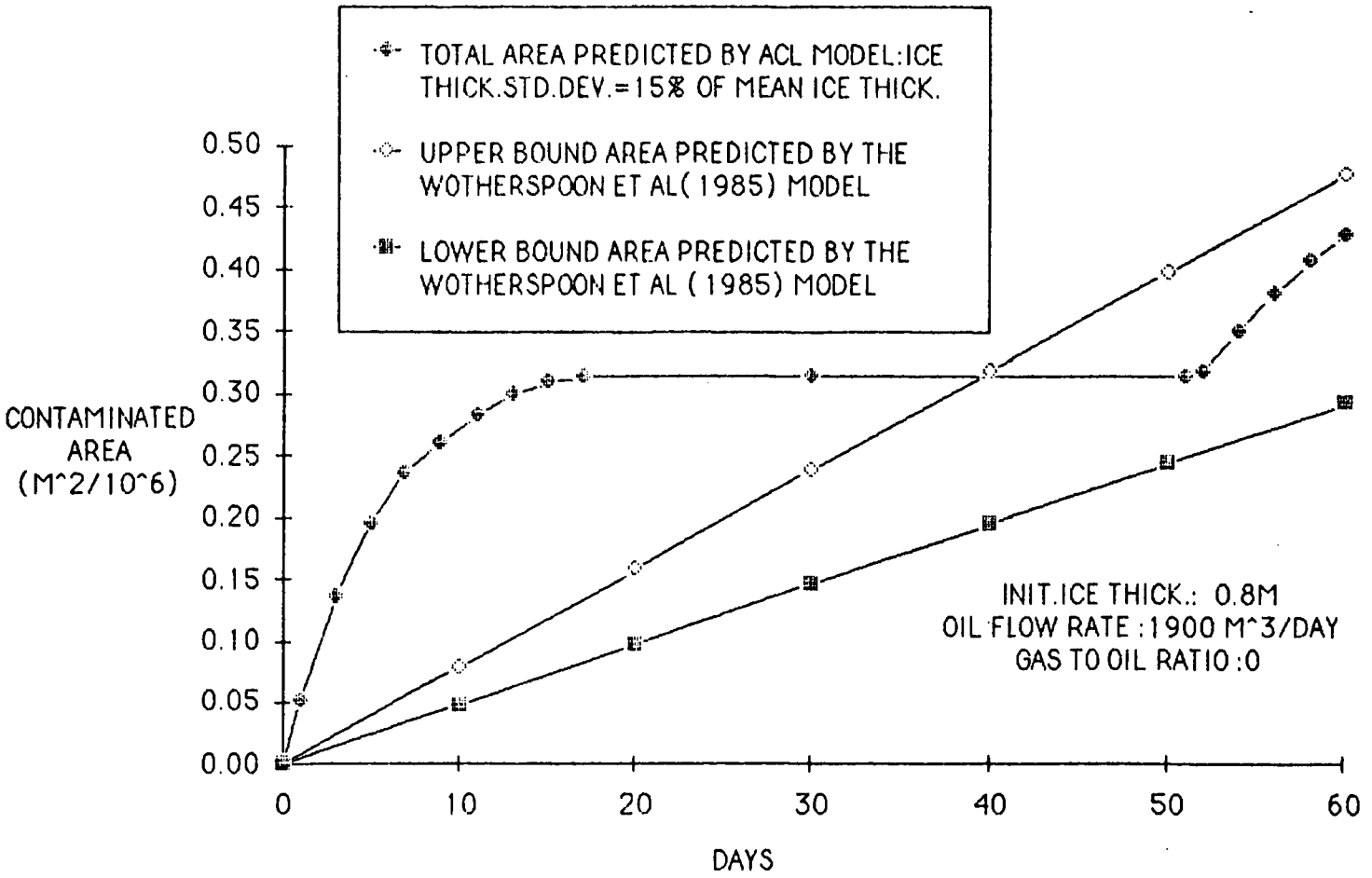

Figure 11. Comparison of Arctec and Wotherspoon (1985) model predictions of contaminated area for a oil spill under rough ice.

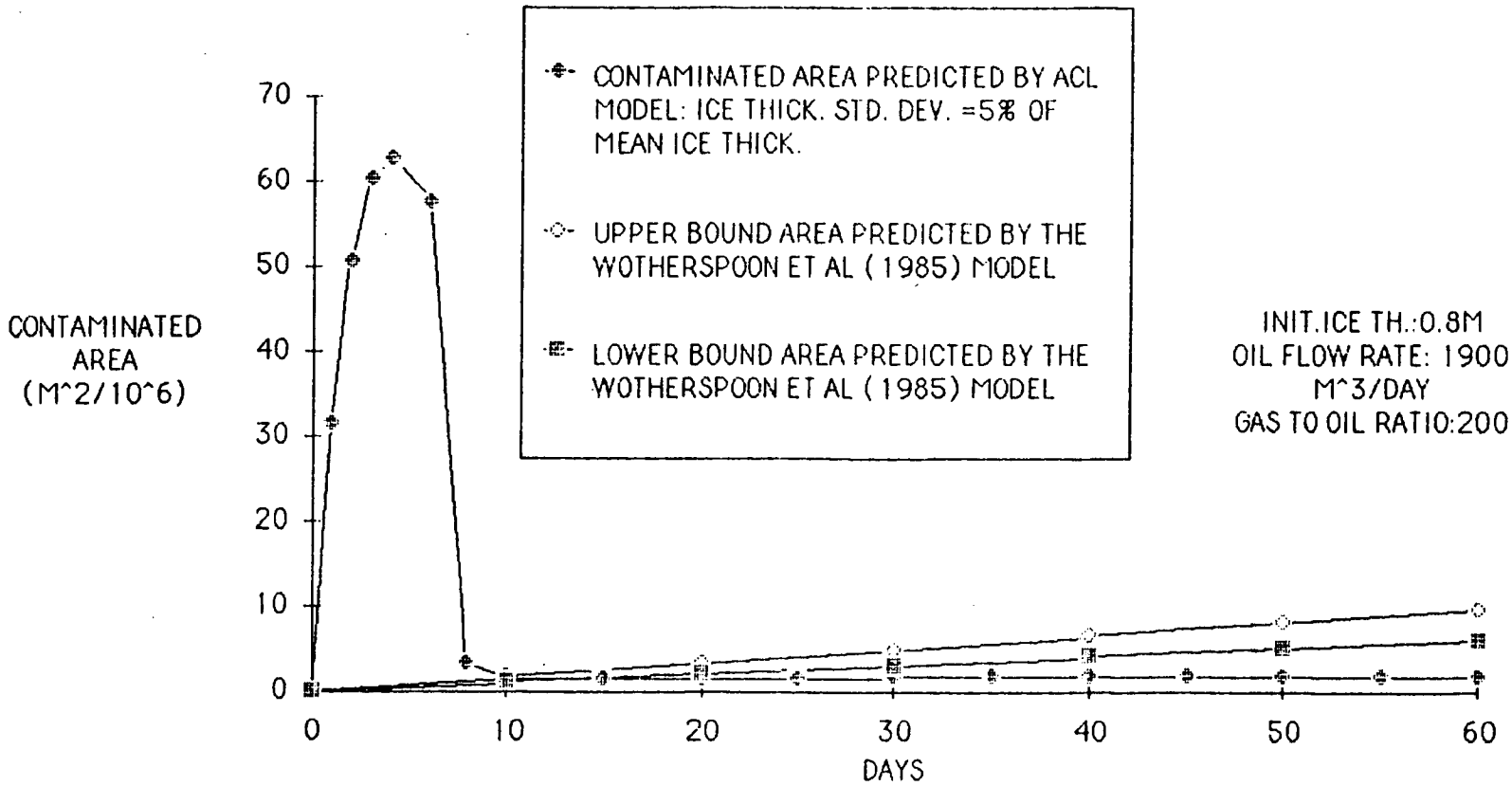

Figure 12. Comparison of Arctec and Wotherspoon (1985) model predictions of contaminated area for a continuous oil and gas spill under smooth ice.

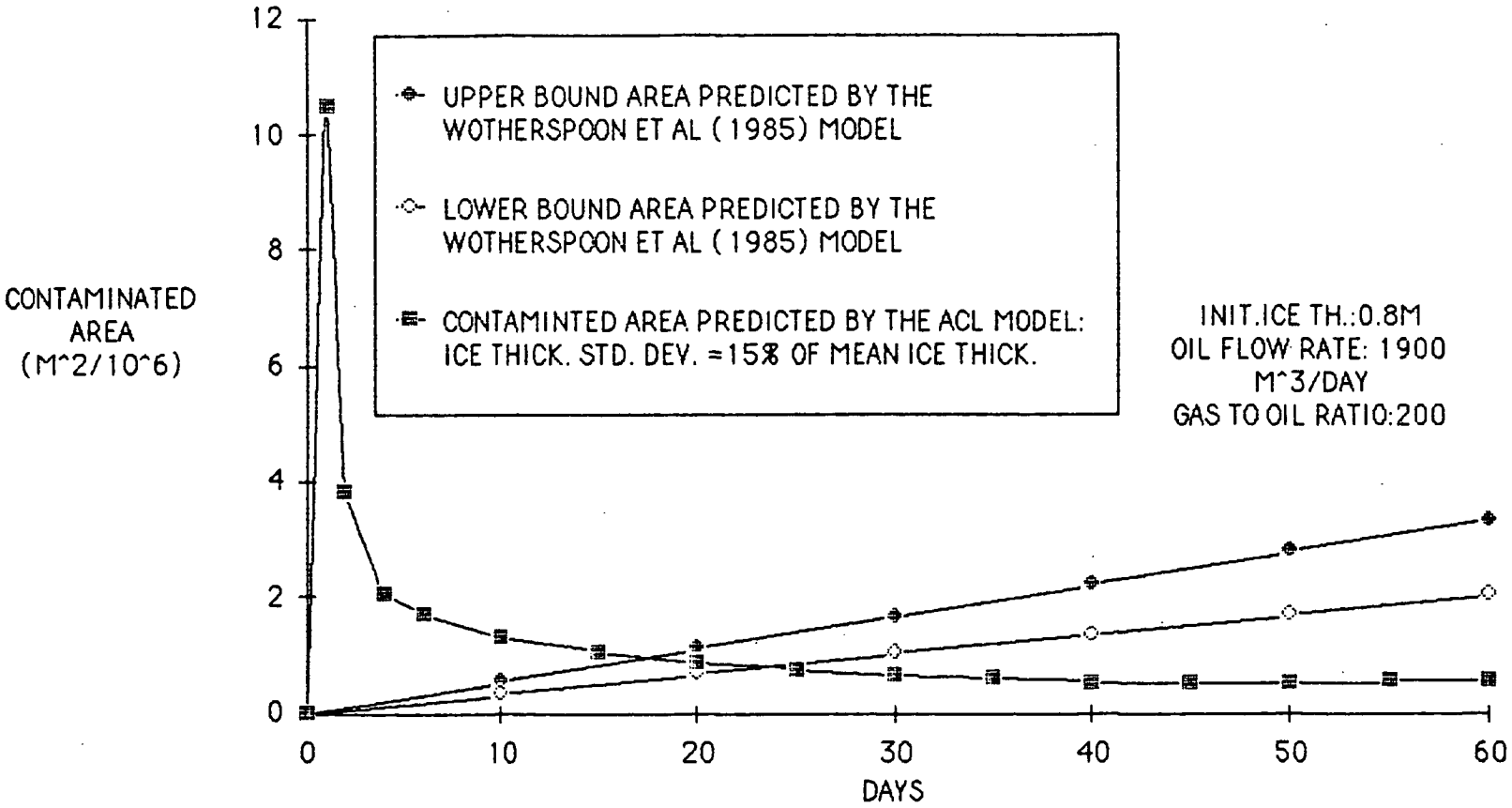

Figure 13. Comparison of Arctec and Wotherspoon (1985) model predictions of contaminated area for a continuous oil and gas spill under rough ice.

The Wotherspoon (1985) model provided a significantly different prediction. Their model predicted the contaminated area to increase linearly with time. This difference reflects variations in approach between the two models. The Arctec model treated ice rupture as a separate event whereas the Wotherspoon (1985) model accounted for the increased spreading of a combined oil and gas discharge by multiplying the contaminated area for an oil-only discharge with a constant spread factor.

UNCERTAINTIES AND RECOMMENDATIONS FOR FUTURE STUDIES

The results of this study are limited by gaps in our understanding in a number of important factors. Additional data are required before a definitive evaluation may be made of the Wotherspoon (1985) model.

A better understanding of the available under-ice storage volume is believed to be most critical for improving the accuracy of spreading analyses. A number of factors contribute to this uncertainty.

There is a general lack of data to define the under-ice storage volume. The available field data consists mainly of linear ice thickness profiles (with the single exception of Kovacs et al (1981). Thus it is necessary to extrapolate the present data to three dimensions to obtain under-ice storage volume estimates. Also, uncertainties remain regarding the nature of the three-dimensional under-ice surface, such as the accessibility of local pits to oil or gas or to both.

The role of skeletal layer voids in sea ice is another factor contributing to this general uncertainty. As discussed, results from the field tests done to date are contradictory in that differing oil-ice skeletal layer interaction processes were observed.

Additional field data are required. Efforts to map the under-ice surface in three dimensions should receive highest priority.

Currents may also limit the available under-ice storage, as they may limit the pool fill depth. This factor remains uncertain as the available data on the effects of currents are primarily applicable to relatively thin oil pool depths.

Finally, the effect of a continuous spill on the formation of a confining ice lip is unclear. This factor has the potential to affect the under-ice storage by influencing the pool fill depth.

REFERENCES

Comfort, G. and R.Y. Edwards. 1978. Ice conditions in Viscount Melville Sound and Barrow Strait West. Arctec Canada Limited. Report 3/5 submitted to Environment Canada. Ottawa.

Comfort, G. 1986. Under-ice roughness measurements. Arctec Canada Limited. Report 2041-II submitted to Environmental Studies Revolving Fund, Ottawa.

Cox, J.C., 1980. The transport and behaviour of oil spilled in and under sea ice. Arctec Incorporated Report 460.

Dickins, D. and I. Buist. 1981. Oil and gas under sea ice. COOSRA Report CV-1.

Herlinveaux, R.H. and B.R. de Lange Boom. 1975. Physical oceanography of the southeastern Beaufort Sea. Beaufort Sea Project Technical Report No. 18. Department of Environment, Victoria, British Columbia.

Hoare, R. 1980. An upward-looking sonar system to profile ice keels for one year. Proceedings, Oceans '80 Conference, Seattle, Washington.

Kovacs, A. 1981. Pooling of oil under sea ice. Proceedings POAC, Quebec City, Quebec.

Kisil, C.A. 1980. A study of oil and gas in fresh and salt water-ice systems. University of Toronto, M.Sc. Thesis, Toronto, Ontario.

Mellor, M. 1983. Mechanical Properties of Sea Ice. CRREL Monograph 83-1.

Milgram, J.H. 1983. Mean flow in round bubble plumes. Journal of Fluid Mechanics, 133: 345-376.

NORCOR 1975. The interaction of crude oil with Arctic Sea ice. Beaufort Sea Project Technical Report No. 27, Department of Environment, Victoria, British Columbia.

NORCOR 1977. Probable behaviour and fate of a winter oil spill in the Beaufort Sea. Environment Canada Report EPS-4-EC 77-5.

NORCOR 1978. A study of ice conditions along marine shipping routes in the Arctic Archipelago. Submitted to Ministry of Transport, Ottawa.

Purves, W. 1978. The interaction of crude oil and natural gas with laboratory-grown saline ice. Arctec Canada Limited, Report 275, submitted to Environment Canada. Ottawa.

Topham, D. 1975. Hydrodynamics of an oil well blowout. Beaufort Sea Project Technical Report No. 33, Department of Environment, Victoria, British Columbia. 52 p.

Topham, D. 1977. The deflection of an ice sheet by a submerged gas source. Transactions of ASME, Journal of Applied Mechanics, 44 Series E (2).

Topham, D. 1980. The interaction of oil with sea ice in an offshore environment. Proceedings Offshore '80s Conference, St. Johns, Newfoundland.

Wotherspoon, P., J. Swiss, R. Kowalchuk, and J. Armstrong. 1985. Oil in ice computer model. Environmental Studies Revolving Funds Report No.19, Ottawa. 129 p.

APPENDIX A

ARCTEC SPREADING MODEL PROGRAM

```
10  REM  SPREAD :OIL-UNDER-ICE ANALYSIS
11  REM  THIS MODEL CALCULATES MODIFIED STORAGES BASED ON ENCAPSU
    LATION
20  DIM R(5,20),D(15,20),TH(5),SA(200),AREA(200)
25  DIM PA(200),PS(200),FD(200),PFD(200)
99  REM  ***
100  REM  ICE FAILURE CRITERION LOOKUP TABLE
101  REM ***
110  REM  ICE THICKNESS (M)
120  READ TH(1),TH(2),TH(3),TH(4)
130  DATA  0.5,1.0,1.5,2.0
140  REM  CRIT.GAS BUBBLE RADII(M) FOR ICE THICK.=0.5,1.0,1.5,2.0
    M
150  FOR I = 1 TO 4
160  READ R(I,1),R(I,2),R(I,3),R(I,4),R(I,5),R(I,6),R(I,7),R(I,8)
    ,R(I,9),R(I,10),R(I,11)
170  DATA  20,40,60,69,79,119,159,198,238,278,317
180  DATA  33,67,100,116,133,200,266,333,399,466,532
190  DATA  45,90,136,158,181,271,361,452,542,632,723
200  DATA  56,112,168,196,224,336,448,560,672,784,896
210  NEXT I
215  REM  CRIT.GAS BUBBLE DEPTH(CM) FOR ICE THICK=0.5,1.0,1.5,2.0
     M
220  FOR I = 1 TO 12
230  READ D(I,1),D(I,2),D(I,3),D(I,4),D(I,5),D(I,6),D(I,7),D(I,8)
    ,D(I,9),D(I,10),D(I,11)
232  REM   ICE STRENGTH=350 KPA
235  DATA  5.28,4.28,4.05,3.98,3.73,3.17,2.98,2.89,2.84,2.80,2.77

240  DATA  7.40,6.02,5.70,5.60,5.25,4.46,4.19,4.07,4.00,3.94,3.90

245  DATA  9.10,7.40,6.99,6.88,6.44,5.48,5.15,4.99,4.91,4.84,4.79

250  DATA 10.54,8.54,8.08,7.94,7.45,6.33,5.94,5.77,5.67,5.59,5.54

255  REM  ICE STRENGTH = 200 KPA
260  DATA  3.06,2.48,2.34,2.30,2.16,1.84,1.72,1.68,1.64,1.62,1.60

265  DATA  4.22,3.42,3.26,3.20,3.00,2.54,2.40,2.32,2.28,2.26,2.22

270  DATA  5.20,4.22,3.99,3.93,3.68,3.14,2.94,2.86,2.80,2.76,2.74

275  DATA  6.00,4.88,4.62,4.54,4.26,3.62,3.40,3.30,3.24,3.20,3.17

282  REM   ICE STRENGTH=100 KPA
285  DATA  1.53,1.24,1.17,1.15,1.08,0.92,0.86,0.84,0.82,0.81,0.80

287  DATA  2.11,1.71,1.63,1.60,1.50,1.27,1.20,1.16,1.14,1.13,1.11

289  DATA  2.60,2.10,2.00,1.97,1.84,1.57,1.47,1.43,1.40,1.38,1.37

291  DATA  3.00,2.44,2.31,2.27,2.13,1.81,1.70,1.65,1.62,1.60,1.58

295  NEXT I
305  INPUT "ENTER OIL FLOW RATE (M^3/DAY)";RO
```

```
307  INPUT "ENTER GAS TO OIL RATIO :";RT
310  INPUT "ENTER ICE THICKNESS (M)";IT
312  INPUT "ENTER ICE THICK.STD.DEV(% OF MEAN THICK)";SD
315  INPUT "ENTER GAS DISS.RATE(M^3/M^2/DAY)-ENTER 1 FOR DEFAULT
   VALUE";DR
320  IF DR = 1 THEN DR = 0.00015
399  REM  ***
400  REM   SPREAD CALCULATIONS
401  REM  ***
405 FL = 350
407 SLOT = 1
409 WRITE = 49312 + 256 * SLOT
410  PR# 1: POKE 1656 + 1,80: PRINT  CHR$ (12)
430  PRINT "                ***   SPREADING OF OIL AND/OR GAS UNDE
   R ICE   ***"
435  PRINT
440  PRINT "INITIAL VALUES AND CONSTANTS :"
445  PRINT "START.ICE THICK.(M):";IT;"  ICE THICK.STD.DEV.(%):";S
   D:"  ICE STRENGTH (KPA):";FL
450  PRINT "OIL FLOW RATE(M^3/DAY):";RO;".GAS TO OIL RATIO :";RT;
   "GAS DISS.(M^3/M^2/DAY):";DR
455  PRINT
460  PRINT "DAY    ICE     TOTAL       TOTAL       FREE        TOTAL
        ACTIVE      OIL     GAS"
465  PRINT "      THICK  OIL DIS.  GAS DIS.    GAS VOL.       AREA
         AREA      THICK  THICK"
470  PRINT "       (M)     (M^3)     (M^3/1000)  (M^3/1000)  (M^2/1000
   )   (M^2/1000)   (CM)    (CM)"
480  IF SF = 1 THEN FL = 350
485  IF SF = 2 THEN FL = 200
490  IF SF = 3 THEN FL = 100
495 VFLG = 0:TFLG = 0
496 ASUM = 0
497 ST = 0.3 * SD * IT / 100
498 OF = 0:GF = 0
499 PV = 0:VP = 0
500  FOR N = 1 TO 1000
509  REM  ***
510  REM  ICE GROWTH CONSTANTS(M/DAY)
511  REM  ***
520  IF IT < 0.9 AND IT >  = 0.5 THEN IG = 0.010
530  IF IT < 1.4 AND IT >  = 0.9 THEN IG = 0.0083
540  IF IT < 1.6 AND IT >  = 1.4 THEN IG = 0.0067
550  IF IT < 1.75 AND IT >  = 1.6 THEN IG = 0.0050
560  IF IT >  = 1.75 THEN IG = 0.003
570  IF IT > 1.81 THEN 1650
580  IF IT >  = 1.75 THEN TFLG = 1: REM  TEMP.FLAG SET TO ALLOW G
   AS DISS.
590 IT = IT + IG
592 MAXT = IT + 2 * SD * IT / 100
593 MI = IT - 2 * SD * IT / 100
594 IR = MAXT - MI
600  IF VFLG = 0 THEN K3 = 1.0: REM  ALL GAS RETAINED IF VENT FLA
   G=0
610  IF VFLG = 1 THEN K3 = 0.2: REM  80% OF GAS VENTED IF VENT FL
   AG=1
620 SN = 0.3 * SD * IG / 100
630 ST = ST + SN
640 OT = RO * N: REM  TOTAL OIL RELEASED
650 GT = OT * RT: REM  TOTAL GAS RELEASED
655 OF = OF + RO:GF = GF + RO * RT
660 GV = GF * (1 - K3): REM  VOL.OF GAS VENTED
670 GF = GF - GV: REM  FREE GAS VOL.AFTER VENTING
679  REM  ***
680  GOSUB 2000: REM  CALCULATE STORAGGE AND AREA
681  REM  ***
```

```
690  IF TFLG = 0 THEN GD = 0: REM  NO GAS DISS.IF TEMP FLAG=0
700  IF TFLG = 1 THEN GD = ACT * DR: REM  GAS DISS.AT RATE IF TEM
   P FLAG=1
710 GF = GF - GD
720  IF GF < 0 THEN GF = 0
730 MOFT = OF / ACT: REM  MEAN OIL FILM THICKNESS
740 BD = GF / ACT: REM  MEAN GAS BUBBLE DEPTH
750 BR =  SQR (ACT / 3.14159): REM  GAS BUBBLE RADIUS
759  REM  ***
760  REM  ICE RUPTURE CHECK
761  REM  ***
770  IF VFLG = 1 THEN 1240
775  IF RT = 0 THEN 1240
780  IF IT < 1.0 AND IT >  = 0.5 THEN J = 1
790  IF IT < 1.5 AND IT >  = 1.0 THEN J = 2
800  IF IT < 2.0 AND IT >  = 1.5 THEN J = 3
810  IF IT >  = 2.0 THEN J = 4
820  IF FL = 350 THEN M = J
825  IF FL = 200 THEN M = J + 4
830  IF FL = 100 THEN M = J + 8
850 P1 = 11:P2 = 11
860  FOR I = 1 TO 11
870  IF BR < R(J,I) THEN P1 = I - 1
880  IF BR < R(J,I) THEN 900
890  NEXT I
900  FOR I = 1 TO 11
910  IF BR < R(J + 1,I) THEN P2 = I - 1
920  IF BR < R(J + 1,I) THEN 940
930  NEXT I
940  IF P1 = 0 AND P2 = 0 THEN 1150
950  IF P1 = 11 THEN D(M,P1 + 1) = D(M,P1)
960  IF P2 = 11 THEN D(M + 1,P1 + 1) = D(M + 1,P1)
970  IF P1 = 11 AND P2 = 11 THEN 1100
980  IF P1 = 11 AND P2 < 11 THEN R(J,P1 + 1) = BR
1000 CH = (D(M,P1) - D(M,P1 + 1)) * (BR - R(J,P1)) / (R(J,P1 + 1)
   - R(J,P1))
1010 B1 = D(M,P1) - CH
1015  IF P2 = 0 THEN B2 = D(M + 1,1)
1020  IF P2 = 0 THEN 1050
1030 CH = (D(M + 1,P1) - D(M + 1,P1 + 1)) * (BR - R(J,P1)) / (R(J
   + 1,P1 + 1) - R(J + 1,P1))
1040 B2 = D(M + 1,P1) - CH
1050 CH = (B2 - B1) * (IT - TH(J)) / (TH(J + 1) - TH(J))
1060 BCRIT = (B1 + CH) / 100
1070  GOTO 1200
1100 B9 = D(M + 1,P1) - D(M,P1)
1101 B8 = IT - TH(J)
1102 B7 = TH(J + 1) - TH(J)
1103 BCRIT = D(M,P1) + B9 * B8 / B7
1110 BCRIT = BCRIT / 100
1120  GOTO 1200
1150 BCRIT = (D(M,1) - D(M + 1,1)) * (IT - TH(J)) / (TH(J + 1) -
  TH(J))
1160 BCRIT = BCRIT / 100
1170  GOTO 1200
1200  IF BD < BCRIT THEN 1240
1210 VFLG = 1
1220 KJ = 0.2
1240  GOTO 1500
1500  REM  ***
1504  REM  PRINT RESULTS
1505  REM  ***
1510  CALL WRITE:N;IJ;"  ";IT;F5.2;"  ";OT / 1000;F8.1;"  ";GT /
   1000;F9.1;"  ";GF / 1000;F9.1;"  ";ASUM / 1000;F10.1;"  ";ACT
    / 1000;F10.1;"  ";MOFT * 100;F5.1;"  ";BD * 100;F5.1:
1520  CALL WRITE: CHR$ (13):
```

```
1564  IF N = 80 THEN  STOP
1600  NEXT N
1650  NEXT SF
1700  END
1999  REM  ***
2000  REM  STORAGE
2001  REM ***
2010 VD = GF + OF:LR = 2 * IG
2020  FOR I = 1 TO N
2030 PA(I) = AR(I)
2040 PS(I) = SA(I)
2050 PF(I) = FD(I)
2060  NEXT I
2080  IF AFLG = 0 THEN NS = N
2100  FOR I = 1 TO N
2110  IF I = N THEN FD(I) = IT:MU = 1: GOTO 2180
2120  IF I <  = NS THEN FD(I) = PFD(I) + LR
2130  IF AFLG = 1 AND I > NS THEN FD(I) = PFD(I - 1)
2135 X = FD(I) - MI
2140  IF X < 0 THEN MU = 1: GOTO 2180
2150 MU = (((X) / IR) / 0.5) ^ 2.7
2160  IF FD(I) > MAXT THEN MU = (2) ^ 2.7
2170  IF FD(I) < IT THEN MU = 1
2180 SA(I) = ST * MU
2190  NEXT I
2500 VS = 0
2510  FOR I = 1 TO NS
2520 VP = VS
2530 VS = VP + AR(I) * SA(I)
2550  NEXT I
2610 C = NS + 1:E = N - 1
2620  FOR I = C TO E
2630 VP = VS
2640 VS = VP + AR(I) * SA(I)
2650  NEXT I
2700  IF VD >  = VS THEN AFLG = 0
2710  IF VS > VD THEN AFLG = 1
2740 VS = 0
2750  FOR I = 1 TO NS
2760 VP = VS
2770 VS = VP + AR(I) * SA(I)
2780  IF VS > VD THEN NS = I: GOTO 2999
2790  NEXT I
2800 C = NS + 1:E = N - 1
2810  FOR I = C TO E
2820 VP = VS
2830 VS = VP + AR(I) * SA(I)
2840  IF VS > VD THEN NS = I: GOTO 2999
2850  NEXT I
2999  REM  ***
3000  REM  AREAS
3001  REM  ***
3002  REM  INCREASING AREA CASE
3010  IF AFLG = 1 THEN 3500
3020 AREA(N) = (VD - VS) / SA(N)
3030 AS = AS + AR(N)
3040 ACT = AS
3400  GOTO 4000
3500  REM  DECREASING AREA CASE
3510 AREA(NS) = (VD - VP) / SA(NS)
3520 ACT = 0
3530  FOR I = 1 TO NS
3540 ACT = ACT + AR(I)
3550  NEXT I
3560  IF ACT >  = ASUM THEN AS = ACT
3590  IF N = 1 THEN 4000
```

```
3600 AREA(NS + 1) = PA(NS) - AREA(NS)
3610  IF NS = N - 1 THEN 4000
3620 C = NS + 2
3630  FOR I = C TO N
3640 AR(I) = PA(I - 1)
3650  NEXT I
4000  RETURN
```